DAWOUD, UTHMAN MOHAMMED

APPLICATION OF ELECTROCHEMICAL TECHNIQUE TO MEASURE MASS TRANSFER OF MACROMOLECULES IN A FLOW SYSTEM

The University of Oklahoma PH.D. 1980

THE UNIVERSITY OF OKLAHOMA

GRADUATE COLLEGE

APPLICATION OF ELECTROCHEMICAL TECHNIQUE TO MEASURE MASS TRANSFER OF MACROMOLECULES IN A FLOW SYSTEM

A DISSERTATION

SUBMITTED TO THE GRADUATE FACULTY

in partial fulfillment of the requirements for the degree of

DOCTOR OF PHILOSOPHY

BY

UTHMAN MOHAMMED DAWOUD

Norman, Oklahoma

1980

APPLICATION OF ELECTROCHEMICAL TECHNIQUE TO

MEASURE MASS TRANSFER OF MACROMOLECULES

IN A FLOW SYSTEM

APPROVED BY

John M. Rodovich

Carl E. Locke

Robert G. Wills

John E. Francis

DISSERTATION COMMITTEE

TABLE OF CONTENTS

Page

APPENDICES

LIST OF TABLES

LIST OF FIGURES

Figure Page

ACKNOWLEDGEMENTS

The author is grateful to all who gave assistance in the work leading to the completion of this dissertation. A special note of thanks is due to Dr. John M. Radovich, who served as chairman of the dissertation committee. Also, I would like to thank Drs. Carl E. Locke, Sam S. Sofer, Robert A. Wills and John Francis for their participation as members of the committee.

Gratitude is also due to the University of Petroleum and Minerals in Saudi Arabia and Chemical Engineering Department at the University of Oklahoma for its financial support.

Several people gave valuable assistance in building the experimental apparatus and solving various related problems. These individuals include:

Dr. Glenn Dryhurst
Dr. C. Leroy Blank
John Noe
Peter Lin
K. Hudson
Mark Southard
Lionel Karber
Bahman Behnam

Finally, I wish to thank my wife and my two children for their support all through my graduate studies.

ABSTRACT

The electrochemical technique was used to study the mass transfer rates of macromolecules in a flow system. The direct oxidation of NADH was the electrolytic reaction. The flow system consisted of rectangular duct. Glassy carbon disc electrodes were used as the working electrodes. A platinum sheet was used as the counter electrode, and the reference electrode was Ag/AgCl.

The Reynolds numbers were 7174, 10782, and 14307. The Schmidt number was held constant at 4730.

Steady state voltammetry and the scanning methods were used to obtain voltammograms (current-potential curves) with well defined mass transfer regions.

The experimental local mass transfer coefficients (k's) were 2.43×10^{-3}, 3.15×10^{-3}, and 3.35×10^{-3} cm/sec at Re = 7174, 10782, and 14307 respectively. These experimental values of k's were compared with the literature by using the expression,

$$St = \frac{k}{v} = 0.0165\ Re^{-0.14}\ Sc^{-0.67}$$

The discrepancy among the experimental and literature-based values was in the range of 46% to 62%. This is due to the fact that the correlations cited in the literature were developed for smaller molecules.

APPLICATION OF ELECTROCHEMICAL TECHNIQUE TO MEASURE MASS TRANSFER OF MACROMOLECULES IN A FLOW SYSTEM

CHAPTER I

BACKGROUND

Introduction

In reverse osmosis, the performance of a given membrane system in terms of solute separation and permeate flux is evaluated by comparison of the pure water and solute permeabilities and the mass transfer coefficient on the high pressure side[1,2]. This mass transfer coefficient characterizes the flow conditions of the feed past the membrane, i.e., the liquid phase resistance. In terms of the film theory of mass transfer through this liquid boundary layer, the mass transfer coefficient is needed to determine the solute concentration at the surface[3-7]. Once this concentration is known, polarization and the true membrane retention can be calculated. In the gel polarization model for ultrafiltration, the limiting flux at steady state is calculated on the basis

of mass transfer of solute from the membrane surface (at fixed concentration) back into the bulk solution[8-11]. If the flux and mass transfer coefficient are known, the concentration at the membrane can be found.

Ultrafiltration and reverse osmosis, in addition to their initial use for water desalination, are used in the laboratory, and in the food processing, pharmaceutical, chemical, medical, waste treatment and paper and pulp industries[12-20]. Reverse osmosis and ultrafiltration are also important on the biological level because of their common occurrence in many organs of the body. In any membrane process, the membrane permeability is necessary for determining the transport rate of a given component through the membrane. In reverse osmosis and ultrafiltration, the existence of liquid boundary layers on either side of the membrane precludes direct calculation of the intrinsic membrane permeability. The importance of the liquid phase resistances has long been known and must be accounted for when determining the membrane permeability from experimental measurements of overall transport resistance[21-25].

In all cases, the mass transfer coefficient (k) is the one which would be calculated for mass transfer for the same flow geometry and Reynolds number without membrane permeation. The mass transfer correlations which express k in terms of flow geometry, fluid velocity

and the solute properties, are derived from heat-mass transfer analogies, or from experimental data for small solutes. Gill et al.[26], Murkes and Bohman[27], and Kwang and Kammermeyer[28] have presented summaries of these correlations. However, for macromolecules (> 500 MW), the equations only give a qualitative picture of the flux behavior. They cannot be used to accurately predict ultrafiltration fluxes[29-31]. Mass transfer correlations based on experimental data for macromolecules should increase the accuracy of these predictions. Accuracy in designing ultrafiltration systems is becoming increasingly more important in view of the widespread uses of the process. The development of a technique for measuring the liquid-phase mass transfer rates of macromolecules will provide the required experimental data. Knowledge of their liquid-phase mass transfer coefficients will lead to a more fundamental understanding of membrane separation processes for macromolecules.

Our general goal is to develop an inexpensive and suitable technique to measure the mass transfer rates of large molecules in solutions. Since the macromolecules processed in membrane separations are often biological in nature (e.g. proteins), our choice of techniques was also oriented toward methods which could be adapted to such solutes. To our knowledge, no data for applications of the available mass transfer techniques

to macromolecules has been reported in the literature. The most widely used techniques are dissolution and sublimation, profilometry and holographic interferometry, adsorption and electrochemical.

Our results might find wide application in biological and biochemical engineering. Tubular reactors with immobilized enzymes attached to the inner walls are one application. In such reactors, the rate of reaction depends on the rate of the mass transfer to the wall. Bailey and Ollis[32], and Wingard et al.[33] have discussed the features of these reactors and their applications. Kobyayashi and Laidler[34] have also discussed the theory of such reactors. Some of these applications are: 1) the production of pure L-amino acids which can be used in medicine and the food industry; 2) the production of cofactors such as NAD or NADP[35-38] which can be used in affinity chromatography. Other applications involve the study of body fluids. It is possible to study the concentration of glucose in blood, to study permeability of pulmonary capillaries to sucrose, to study lipid metabolism and transport which causes atherogenesis disease. The etiology of this disease is due to the deposition of cholesterol in the neighborhood of bends or junctions. The latter act as turbulence promoters which will create wake regions and the deposition of blood particulates will be enhanced at these regions. Our experimental

model can represent any part of the vascular system or compartment on the assumption that the vascular system is a rigid tube and the bends or junctions can be represented by simply shaped obstructions or inserts. Middleman[39] has given a comprehensive analysis of such systems.

Dissolution Technique and Sublimation Technique

Mass transfer rates are determined from the dissolution and sublimation techniques by relating the mass transfer coefficient (k) to the weight loss of solid and the elapsed time. The solute is cast in a solid form which is then placed in the fluid. Examples of this are dissolution of benzoic acid in water solution[40-42] and sublimation of napthalene in air[43]. Only average mass transfer coefficients can be determined from these measurements. Development of surface roughness and fissures[44] during dissolution/sublimation, and sample contamination during handling introduce error into the results. In addition, renewal of the test specimen each time is necessary.

Profilometric Technique

Profilometric methods are based on measurements of the geometric changes that occur in a solid as a result of mass transfer. Overall mass transfer coefficients for

cast napthalene[45]; local coefficients for acenapthene cylinders[46] and napthalene-coated rods[47] are examples of this method. MacLeod and Todd[48] developed a variation of this method by using an insoluble polymer as a surface coating. This coating, which is impregnated with a soluble swelling agent, undergoes local changes in its degree of swelling in response to mass transfer of the swelling agent. While eliminating the surface roughness problems and need for a new test specimen each time, this variation requires the measurement of many physicochemical properties of the polymer-swelling agent. Point-to-point measurements on the sample are necessary if local coefficients are desired.

When a sublimating substance is used, the change in the level surface must be kept small so the flow over the solid surface remains undisturbed. In case of the polymer coating, the coating recession is on the order of 10^{-6} m[49]. Therefore, the need for a very delicate mechanical means of measurements becomes impractical and laborious. Diffusion of the swelling agent parallel to the surface will cause a systematic error in the mass transfer measurements.

Holographic Interferometry Technique

Kapur and MacLeod have developed holographic interferometry[50,51] for use with profilometric methods to get mass transfer data. Using polymers which are reversibly

swollen by a volatile or soluble swelling agent, they take holograms (double exposure) before and after mass transfer. The set of interference fringes developed by a reference beam shows the local degrees of swelling. Solid-liquid and solid-gas mass transfer rates have been measured in this manner[52,53]. Although more accurate than conventional profilometry, much physico-chemical data is required and diffusion of the swelling agent parallel to the surface might increase the local volumetric changes in the polymer. Thus, the mass transfer rate might not be due to the diffusion in the vertical direction alone. To avoid parallel diffusion, Wild and Uhlenbusch[54] used a stable sublimating substance (camphene) with this technique. In their report, they concluded the interpretation of the fringes for a complicated object is difficult. The nature of the aforementioned techniques and constraints placed on the types of solutes (e.g. cast as solids, polymer-swelling agent) precluded us from considering them for application to solutions of macromolecules.

Adsorption Technique

Since the electrochemical technique is constrained to working with redox systems, the number of macromolecular systems available for study becomes rather limited. We believe that development of an adsorption technique

based on the affinity of a macromolecule for a substrate placed on the walls of a channel would extend our capabilities for measuring the mass transfer of large molecular weight species. Kuncar-Djurdejević[55] used the adsorption of methylene blue on silica gel-coated cylinders to indicate the nature of fluid flow past these objects. He and others later determined the rates of mass transfer by measuring the amount of dye adsorbed on walls of a silica gel-coated tube, with and without turbulence promoters in the flow path[56-59]. Problems with unsatisfactory surface roughness and mechanical stability of the coating have been overcome (peak heights $\simeq 2\mu$ and $Re = 3 \times 10^5$) by adsorbing the silica gel on an oxidized aluminum surface[56]. Cijović and Mitrović also describe the methods for obtaining calibration curves of reflectance vs. concentration of adsorbed species[56]. The only problem associated with this technique is that the test specimen must be renewed each time. However, the technique sounds promising and can be used to study macromolecular systems based on the availability of suitable adsorbents. Such adsorbents may be drawn from the field of adsorption or affinity chromatography.

Electrochemical Technique

The electrochemical technique involves the measurement of electric current at a wall electrode which is part

of an electrolysis cell. The current is generated by reduction or oxidation of a transferring electrolyte at the electrode surface. First developed by Lin et al.[60] for measuring average mass transfer rates in an annulus. Reiss and Hanratty[61] and Van Shaw[62] extended this method to the measurement of fluctuating and local mass transfer rates. The mass transfer coefficients are related to the limiting current. At a given Reynolds number, the limiting current is obtained from a plot (polarization curve) of measured current versus applied voltage. At large enough voltages, the change in current for a unit change in voltage is zero. Under these conditions (Re, applied voltage) the current generated at the electrode is limited by the rate of mass transfer of redox ions to the surface of the electrode. Also, the concentration of redox ions at the surface is zero.

Many studies of mass transfer under laminar and turbulent conditions for a wide range of Schmidt numbers have been reported in the literature[63-65]. A review of many applications has been reported by Mizushina[66]. The versatility of the electrochemical method is illustrated by application to studies of mass transfer in the presence of turbulence promoters[67-69] and in solutions of drag reducing polymer solutions[70-72]. It is interesting to note that in these polymer solutions, the rates of transfer of redox ions was measured, <u>not</u> the rate of transfer of the polymer.

The many advantages and versatility of the electrochemical method make it a likely candidate for adaption to the study of mass transfer of macromolecules. The only problem is that it can only measure the rate of transfer of a redox ion.

CHAPTER II

SELECTION OF THE EXPERIMENTAL SYSTEM

The first objective of this research was to design and describe in detail, the experiments using a flow system which was suitable for measuring mass transfer coefficients of macromolecules. It is clear from the background section that the electrochemical technique, because it avoids surface roughness and renewal of the test section, is the technique for our measurements. The problem is to find a macromolecular system (MW > 500) which undergoes a diffusion — controlled redox reaction. For the first condition, we found[73] that NADH (nicotinamide adenine dinucleotide, reduced) is the compound that met our needs. It can be oxidized according to the following reaction, $NADH \rightarrow NAD^+ + H^+ + 2e$

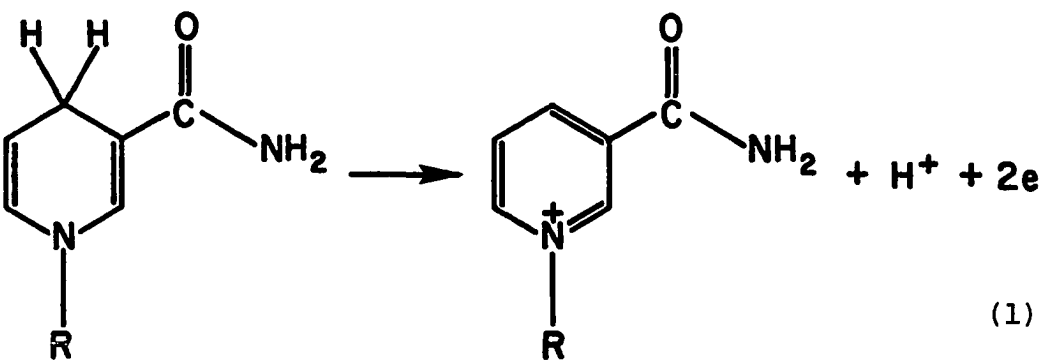

(1)

where R is adenosine diphosphate. This reaction transfers two electrons. The anhydrous molecular weight of NADH is 709.4, (Sigma Chemical Company, #N8129).

NADH also seems especially suited to macromolecular studies because it can be attached to higher molecular weight materials (e.g. polylysine) without the loss of activity[74]. By such attachment, we could easily extend our studies to a homologous series of macromolecules. The second condition can be satisfied by using a large excess of indifferent electrolyte, usually a concentration at least 100-fold higher than that of the electroactive species[73]. A comprehensive study of the NADH system using the electrochemical technique has been reported in the literature[73, 75-83]. Blaedel and Jenkins[80,81] were the first to study the direct electrochemical oxidation (without mediators) of NADH at micromolar levels (10μM) in aqueous solution at glassy-carbon rotating disc electrodes. They produced well-defined, current-potential (voltammograms) curves manually; the technique was called steady state voltammetry (SSV). In SSV, voltammograms are obtained pointwise, by allowing the current transients to die out until the steady state is reached. This procedure eliminated most of the charging current. They also conditioned and pretreated the glassy-carbon disc electrode to clean the electrode surface of any surface functional groups and oxide films that might hinder or slow the reaction.

Moiroux and Elving[81,82] studied the effects of adsorption, electrode material and operational variables on the direct electrochemical oxidation of NADH. They noticed that the NAD^+ produced by the electrochemical oxidation of NADH adsorbed on the electrode. This phenomenon leads to the presence of both the adsorption-controlled and diffusion controlled processes, which is a disadvantage since the two processes produce overlapping voltammograms. Moirous and Elving[82,83] developed procedures which avoid the adsorption process. One way to avoid the adsorption-controlled process is to use an excess amount of NAD^+ with NADH solution. The second way is to cover the electrode surface with NAD^+ first, and then use the covered electrode in the electrochemical oxidation of NADH. They mentioned that the covered electrode should not be held in the range of -0.5 to 0.3v for longer than a few minutes in order to minimize the slow desorption of NAD^+. Also the adsorption is facilitated by decreasing the temperature. This means that at high temperature (25°C or more), the covered electrode is not desirable for practical applications. It was also found[82,83] that the glassy-carbon electrodes have less adsorption problems than any other type of carbon electrodes.

In summary, the electrochemical technique was used in a flow system suitable for measuring the mass transfer of dilute $NADH/NAD^+$ (10μM/20μM) from a bulk

solution to glassy-carbon disc electrodes. The conditioning and pretreatment methods described by Blaedel and Jenkins[80,81] were adopted for cleaning the electrodes. Four Reynold's numbers (Re) of 7174, 10782, 14307, and 24882 were chosen for our investigation. The first three values of Re corresponded to 40, 60, and 80 percent flow on the rotameter with a maximum flow rate of 4 gal/min. The first value of Re = 7174 was within the limit of fully developed turbulent flow. The Re value of 24882 corresponded to 60% flow on a rotameter with a maximum flow rate of 9.4 gal/min. The three Re values of 10782, 14307, and 24882 were selected just to complete our investigation of the flow system. The calculation of the selected flow rates and their corresponding Re and velocities are shown in Appendix A. The working temperature was 26°C.

As part of this research, a flow system suitable for measuring the mass transfer for macromolecule solutions using the electrochemical technique had to be designed. The second goal was to test the performance of flow system by studying the oxidation of dilute solution of NADH and producing voltammograms at the selected flow rates. These topics will be covered in a later section.

CHAPTER III

DATA TREATMENT

Mass Transfer Coefficient

In electrochemical systems, the ions move from the bulk of the solution to the working electrode surface via three types of mass transport processes. These are migration, diffusion, and convection. The total flux N_A of a component A moving in a direction perpendicular to the flow is expressed as[66,84-86],

$$N_A = (J_{mig.})_A + (J_{diff.})_A + (J_{con.})_A \qquad (2)$$

where the J's are the individual fluxes of component A. Also, when mass transfer exists, the electrolysis current (I) is equal to the product of the charge involved in the reaction of one mole of the electroactive species at the working electrode surface and the flux, N_A, of this substance,

$$I = nFA\ N_A \qquad (3)$$

where n is the number of electrons involved in the reaction, F is the Faraday constant and A is the area of the electrode.

The product nF is the charge per mole of the species A[84-86]. The mass transfer coefficient embodied in equations (2 and 3) can be easily calculated if equation (2) is reduced and simplified. The migration term in equation (2) can be eliminated if the reaction is under diffusion controlling conditions. This condition has been achieved by adding a large excess of background or supporting electrolyte[73,86]. The convection term has been eliminated since the reaction shown in equation (1) is a redox one (the mass transfer in the perpendicular direction is by equimolar counter diffusion only), which implies no net flow in the direction perpendicular to the main bulk flow in the flow cell. Therefore equation (2) becomes (Y is in the vertical direction),

$$N_A = (J_{diff.})_A = - D \frac{\partial C_A}{\partial Y} \qquad (4)$$

where D is the diffusion coefficient. The flux is also defined as[87,88].

$$N_A \equiv k(C_b - C_w) \qquad (5)$$

where k is the mass transfer coefficient, C_b is the bulk concentration and C_w is the concentration at the surface of the working electrode. The C_w value depends on the applied potential and is equal to zero at sufficiently

high applied potential under diffusion controlled conditions. At this potential, the electrolysis current reaches a limiting value (plateau) called the limiting current (I_L). Equations (3) and (5) are then combined and solved for the mass transfer coefficient,

$$k = \frac{I_L}{nF\ A\ C_b} \tag{6}$$

The value of k also could be compared by using a suitable correlation from the literature. A well known correlation is the Colburn relation,

$$St = 0.023\ R^{-0.2}\ Sc^{-0.67} \tag{7}$$

where St is the Stanton number ($= \frac{k}{v}$, v is the mean flow velocity), and Sc is the Schmidt number ($= \frac{\nu}{D}$, ν is the kinematic viscosity). Berger and Hau[65], in their investigation of mass transfer in turbulent pipe flow measured by the electrochemical method for ferri-ferrocyanide system, found that the Colburn equation (7) underestimated the value of St at high Schmidt numbers (Sc > 1000). They have developed a correlation for measuring the mass transfer coefficient in fully developed flow in a smooth pipe over the range $8 \times 10^3 < Re < 2 \times 10^5$ and Schmidt numbers varying between 1000-6000. The correlation is

$$St = 0.0165\ Re^{-.14}\ Sc^{-0.67} \tag{8}$$

The range of our Re was between $7 \times 10^3 - 15 \times 10^3$, which is very close to the range given with correlation[8]. The value of Sc for our system was found to be 4730 (see Appendix F) which falls in the range given with correlation[8]. Therefore correlation (8) could be used to compare the experimental value of k obtained by equation (6).

CHAPTER IV

EXPERIMENTAL

Materials

Reduced nicotinamide adenine dinucleotide (NADH #N8129), nicotine adenine dinuecleotide (NAD+ #N7129) and sodium phosphate monobasic (#S0751) and dibasic (#S0876) were obtained from Sigma Chemical Company (St. Louis, MO.) and were used as received. The Bacton Agar (#0140-01) for making agar gel was obtained from Difco Laboratories (Detroit, Michigan). All solutions were prepared with deionized water. All NADH/NAD+ solutions were made fresh each day for each experiment.

Electrodes

The working glassy carbon electrode discs were constructed from 2 cm (length) x 0.3 cm (diameter) rods. The glassy carbon rods were grade GC-20 obtained from IMC Industry (New York, NY 10017). The glassy carbon electrodes were selected because glassy carbon has less adsorption phenomena than any other type of carbon[82,83]. The glassy carbon rods were cemented with super glue into

plastic tubes of 0.185 in. O.D., 0.115 in. I.D. and 3 in. in length. The plastic tubing and the glass carbon surface were ground flush to each other on a rotating polishing wheel using 600-mesh polishing paper disc. The glassy carbon disc electrodes were then polished successively with 23 μ, 8 μ, and 5 μ silicon carbide Ultralap polishing paper discs (Moyco Industries Inc., Philadelphia, PA 11932). The glassy carbon electrode discs were finally fine polished with 0.5 μ Chromium oxide Ultralap polishing paper disc. The working glassy carbon electrode discs were then washed with distilled water and dried with fine tissue paper, and then tested for electrical connection and leakage prior to mounting them in the flow cell.

The reference electrode is a silver-silver chloride (SSCE), dipping into 0.01M KCl. 0.01M KCl was used instead of a higher concentration to avoid the contamination of the test solution by the leakage of the silver chloride[80,81]. The reference electrode compartment was located outside the flow cell. Electrical contact between the test solution in the flow cell and the reference electrode was achieved by using salt bridges. The reference electrode compartment was filled with the background solution which was .05M sodium phosphate. All cited potentials are referred to SSCE (i.e., +0.34V VS NHE).

The counter electrode is a platinum sheet of 1/2 in. x 2 in. x .001 in. which was located in the test section of the flow cell.

Apparatus

The electrochemical measurements for steady state voltametry (SSV) and scanning voltametry were made with a polarographic analyzer (PAR) Model 174A, Princeton Applied Research (Princeton, New Jersey). An x-y recorder, Hewlett-Packard Model 7635B was used with the polarographic analyzer. The electric circuit described by Blaedel[81] was also used with the SSV. The circuit is shown in Figure 1. The voltage source consisted of two 1.35 V mercury cells (Sargent-Welch, RM42R) in series. A ten-turn precision potentiometer controlled the applied potential which was measured by a digital voltmeter (Hewlett-Packard Model 3465B). Currents were measured with a digital picoammeter (Model 480, Keithley Instrument, Cleveland, Ohio). The output of the picoammeter was fed into a one channel strip chart recorder (Model B 5237-5, Houston Instrument, Austin, Texas). The circuit described above was used interchangeably with the two-electrode system (working and reference electrode only) or with the three-electrode system (working, reference and counter electrodes). When the circuit was used with the two-electrode system, the

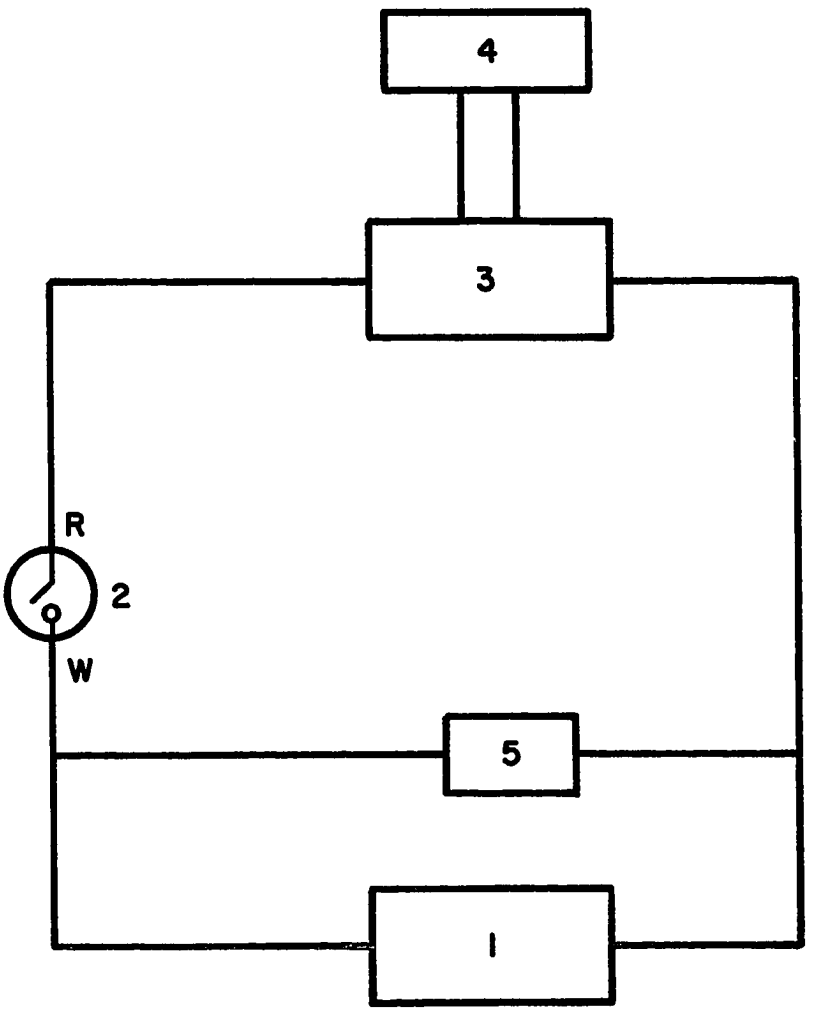

FIGURE 1. Electric circuit for 2-electrode set-up, using steady state voltametry. (1) DC voltage source. (2) flow cell. (3) digital picoammeter. (4) strip chart recorder. (5) digital volt meter. (R) Ag/AgCl reference electrode. (W) glassy carbon working electrode.

digital voltmeter was connected between the working electrode and the common of the voltage source as shown in Figure 1. When the circuit was used with the three-electrode system, the digital voltmeter was connected between the working electrode and the reference electrode as shown in Figure 2.

The 2-electrode system avoids the installation of a counter electrode in the flow system which might disturb the flow pattern in the cell. A simple circuit, such as the one shown in Figure 1, could also be used with the 2-electrode system. In all the studies reported in the literature[75-79,82,83], the 3-electrode system (which allows measurement of the true applied potential) had been used to avoid drawing current into the reference electrode which could shift its potential.

Salt Bridges

Each of the three salt bridges was made of 10 mm O.D. fine fritted discs smoothed flush at one end of the glass tubes of 0.538 in (13.67mm) O.D., 0.422 in. (10.72mm) I.D., and 10 cm in length. The O.D. of the glass tubes, where the fritted disc was mounted, were roughed with a very coarse sand paper to create grooves for cementing the glass tubes with epoxy adhesive in the duct section of the plexiglass sheet. The final O.D.

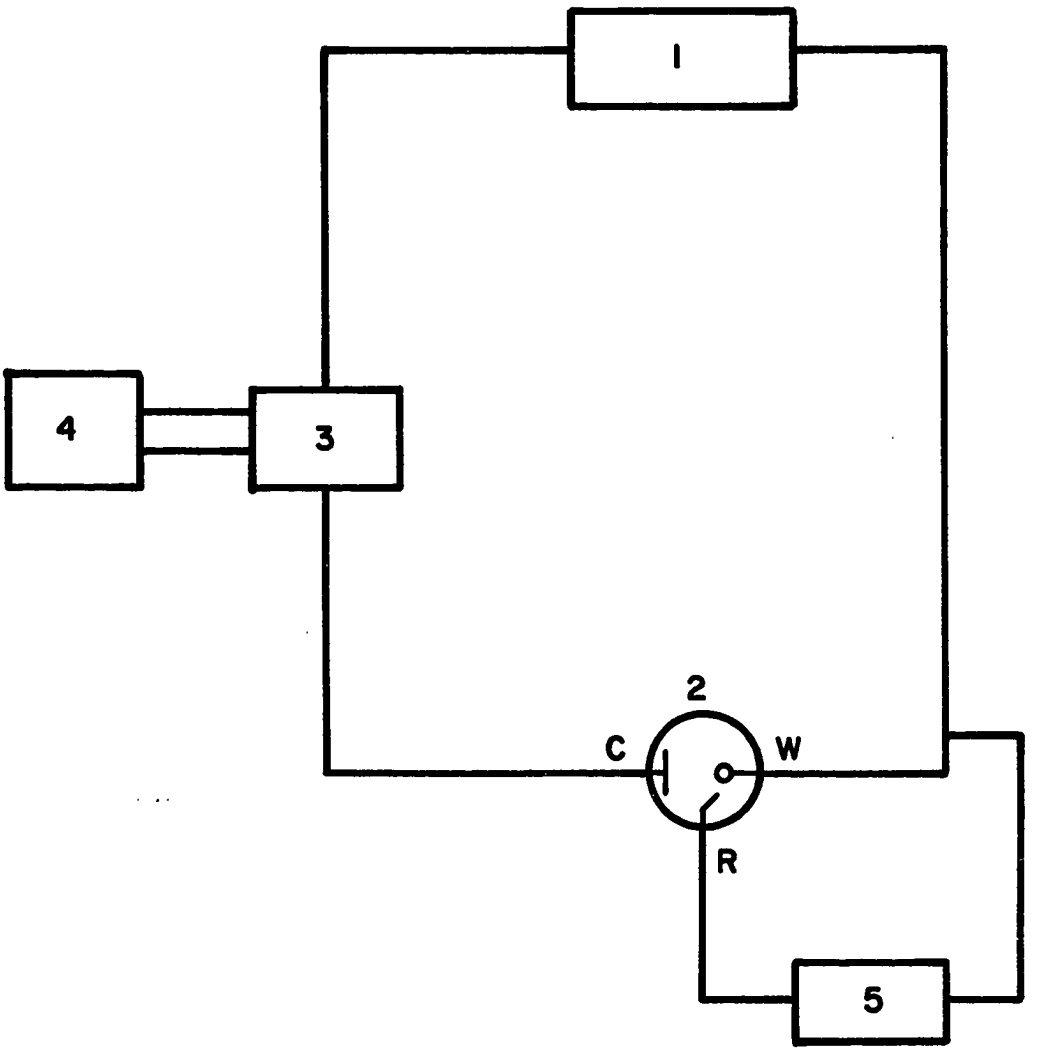

FIGURE 2. Electric circuit for 3-electrode system, using steady state voltammetry. (1) DC voltage source. (2) flow cell. (3) digital picoammeter. (4) strip chart recorder. (5) digital voltmeter. (C) platinum counter electrode. (R) Ag/AgCl reference electrode. (W) glassy carbon working electrode.

of tubes was 0.536 in the glass tubes were filled with agar gel. The agar gel was prepared by warming 4 grams of Bacton agar and 90 ml of the test solution. 0.05M sodium phosphate, pH 9.2 was used instead of the usual KCl to minimize the contamination of the test solution in the flow cell through the agar gel. This solution was cooked in an autoclave to produce a clean, white, homogenous agar solution. The sealed, fritted disc tubes were turned upside down in a vertical position and then filled with the hot agar solution. The tubes were allowed to stand undisturbed in the vertical position until the agar solidified. Four holes of 1 mm dia. were made at the other end of the glass tubes for electrical contact between the agar gel in the tubes and the reference electrode compartment. The three bridges were then cemented with a film of epoxy adhesive and smoothed flush to the test section of the duct. The details of the salt bridge mounted in the duct of the flow cell are shown in Figure 3.

Flow System

The experimental flow system is shown in Figure 4. The flow system was similar to the one described by Youngquist[89] with certain modifications. The modified flow system consisted of a rectangular

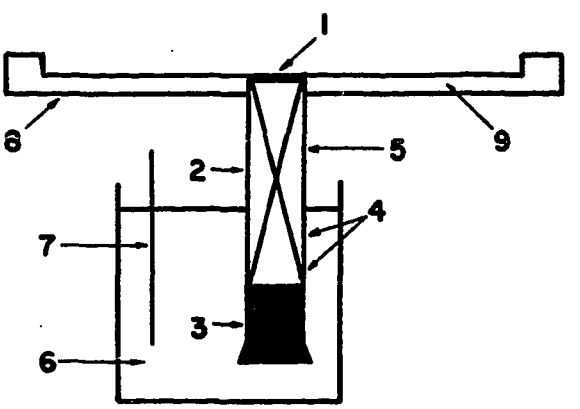

FIGURE 3. Details of salt-bridge mounted in bottom sheet of the flow cell. (1) fine fritted disc. (2) Agar gel plug. (3) cork to hold agar. (4) 1 mm O.D. holes for electrical contact. (5) glass tube. (6) reference solution; 0.05M sodium phosphate pH 9.2. (7) Ag/AgCl reference electrode. (8) bottom sheet of cell. (9) duct in flow cell.

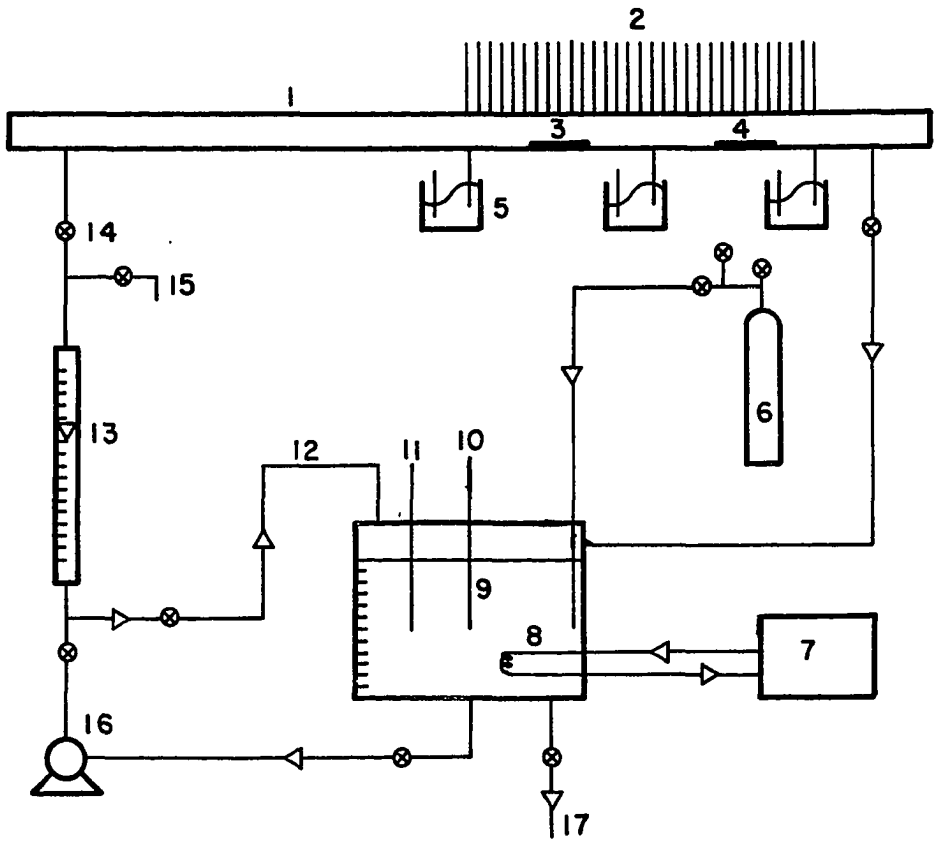

FIGURE 4. Schematic diagram for flow system. (1) flow cell. (2) glassy carbon working electrodes. (3&4) platinum counter electrode. (5) reference electrode compartment (6) nitrogen gas. (7) cooling unit. (8) plastic cooling coil. (9) storage tank. (10) N_2 gas exit. (11) thermometer. (12) by-pass. (13) rotameter. (14) valves. (15) sampling point. (16) pump. (17) drainage.

flow cell through which the test solution was circulated. A one inch I.D. and half inch I.D. schedule 40 PVC pipe, and PVC valves and fittings were used for all connections. The test solutions were recirculated and stored in a 5-gallon plexiglas tank. The test solution was circulated by a seal-less magnetic-drive pump, model AC-5CMD (Cole-Parmer Inst., Chicago, Illinois), with polypropylene impeller and 316 stainless steel shaft. The test solution storage tank contained a plastic cooling coil with coolant to control the temperature of the test solution to within $\pm 0.1^{\circ}C$ of $26^{\circ}C$. The cooling coil was connected to a cooling unit which consisted of a cooling bath, cooler immersion series IC-6 Lauda #13277-120 (Scientific Products, Grand Prairie, Tx), and masterflux tubing pump (Cole-Parmer Inst., Chicago, Illinois) to pump and control the flow of the cooling water to the plastic coil. Two rotameters were used for measuring the flow rates: a Fisher and Porter FP 1-35-G-10 (model 10A 1027A #102727) with stainless steel float and has a maximum flow of 9.4GPM and a Fisher and Porter FP $\frac{1}{2}$-50-G-9 (model 10A 1027A #102722) with stainless steel float and has a maximum flow of 4GPM.

Nitrogen was used to purge the test solution before and during experiments. The by-pass line valve #12 was used to control the flow at the desired Re. Valve #15 was used during calibration of the two rotameters.

Flow Cell

The plexiglass flow cell has a rectangular cross section of 0.635 cm x 2.86 cm. It has a test section length of 11.56 in. (about 29.37 cm). Thirty working, glassy carbon, disc electrodes were located in the cover of the flow cell and they were smoothed flush with the center of the test section. The counter electrode is also located in the test section of the duct. Electrical contact between the test solution in the flow cell and the reference electrode compartment was achieved by the three salt bridges. The first bridge was located at the entrance of the test section and it was used with working electrodes 1 to 8. The second bridge was located in the middle of the test section. It was used with working electrodes 9 to 22. The third one was located at the end of the test section. It was used with working electrodes 23 to 30. This arrangement was made to reduce some of the IR drop in the circuit. The test section of the flow cell was preceded by a section 82.71 cm (32.563 in.) long which was more than 50 diameters (79.53 cm). This assured fully developed flow at the entrance of the test section for all Reynolds numbers.

Flow Cell Assembly

The flow cell was made of two plexiglas sheets. A cover sheet of 4 in. x 50½ in. x ½ in. (10cm x 128cm x 1.27 cm) and a bottom sheet of 4 in. x 50½ in. x 3/4 in.

(10 cm x 128 cm x 1.91cm). In the bottom sheet, a duct 0.635 cm deep, 2.86 cm wide and 118 cm in length was milled. In the test section (which was 11.56 in. from the exit of the duct), two additional slots of ½ in. x 2 in. x .002 in. was milled to accommodate the platinum, counter electrode sheets. The two slots were 4 in. apart. Two holes were made in these slots to fit 16-gauge copper wires for electrical connections. The 16-gauge copper wires were glued in the two holes, by super glue, such that 2 mm of the depth of the hole towards the duct was filled with mercury to make electrical contact between the counter electrode and the 16-gauge wires. The two platinum counter electrodes were then secured in the two slots using super glue. Three holes of 0.55 in (1.4 cm) dia. were also made in the test section of the duct: at the entrance of the test section, in the middle, and at the end of the test section. These holes accommodated the three salt bridges for the electrical contacts between the reference electrode compartments and the test solution. Two holes of 3/4 in. dia. were made at both ends of the duct for inlet and exit of the circulating fluid. The details of the bottom sheet of the flow cell are shown in Figures 5 and 6.

Thirty holes of 0.185 in. dia. were made in the cover sheet of the flow cell to accommodate thirty glassy carbon working electrodes. These holes were located in

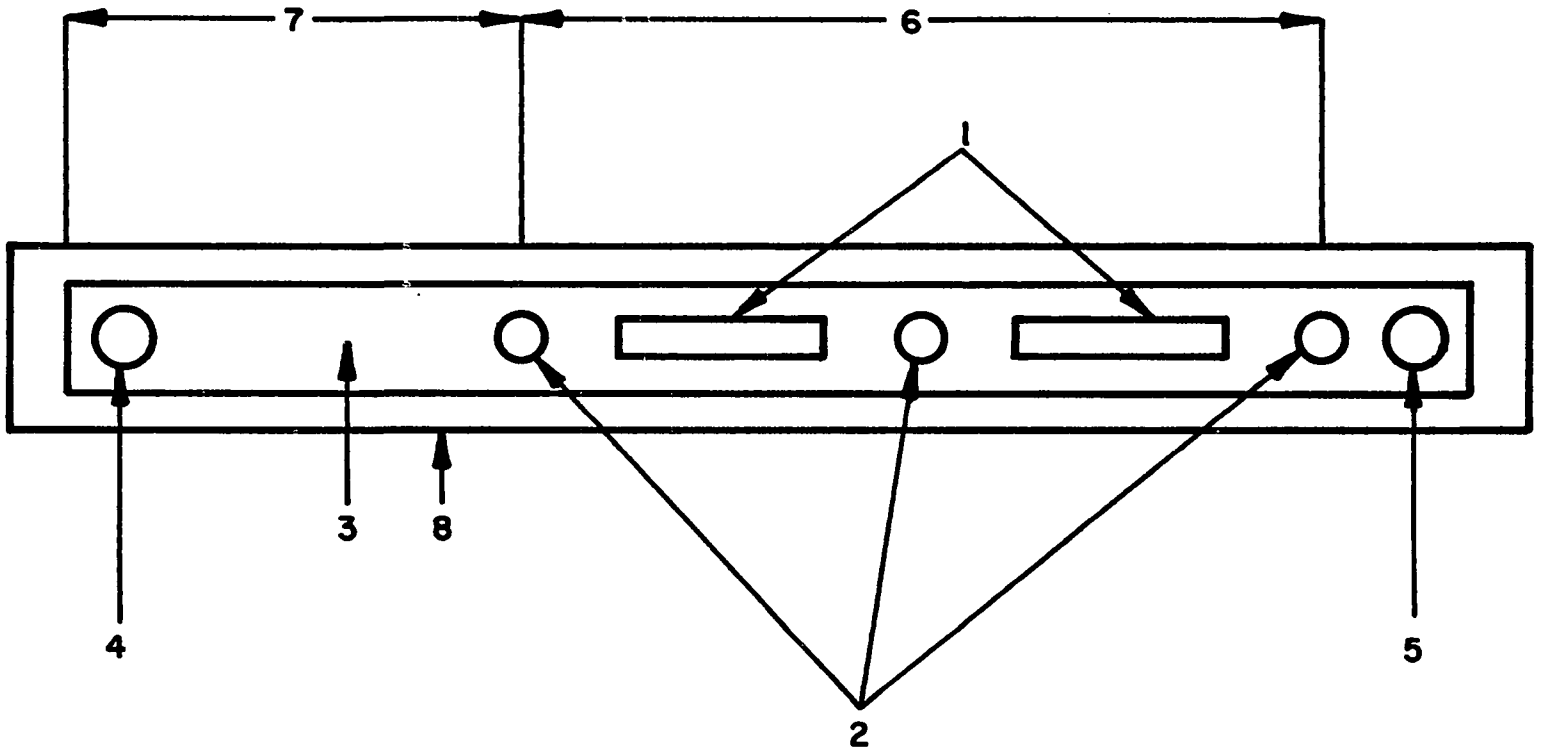

FIGURE 5. Details of bottom sheet in the flow cell. (1) platinum counter electrodes. (2) salt bridges. (3) duct for flow. (4) inlet of duct. (5) exit of duct. (6) test section in duct. (7) preceding section for flow to be fully developed. (8) bottom sheet of flow cell.

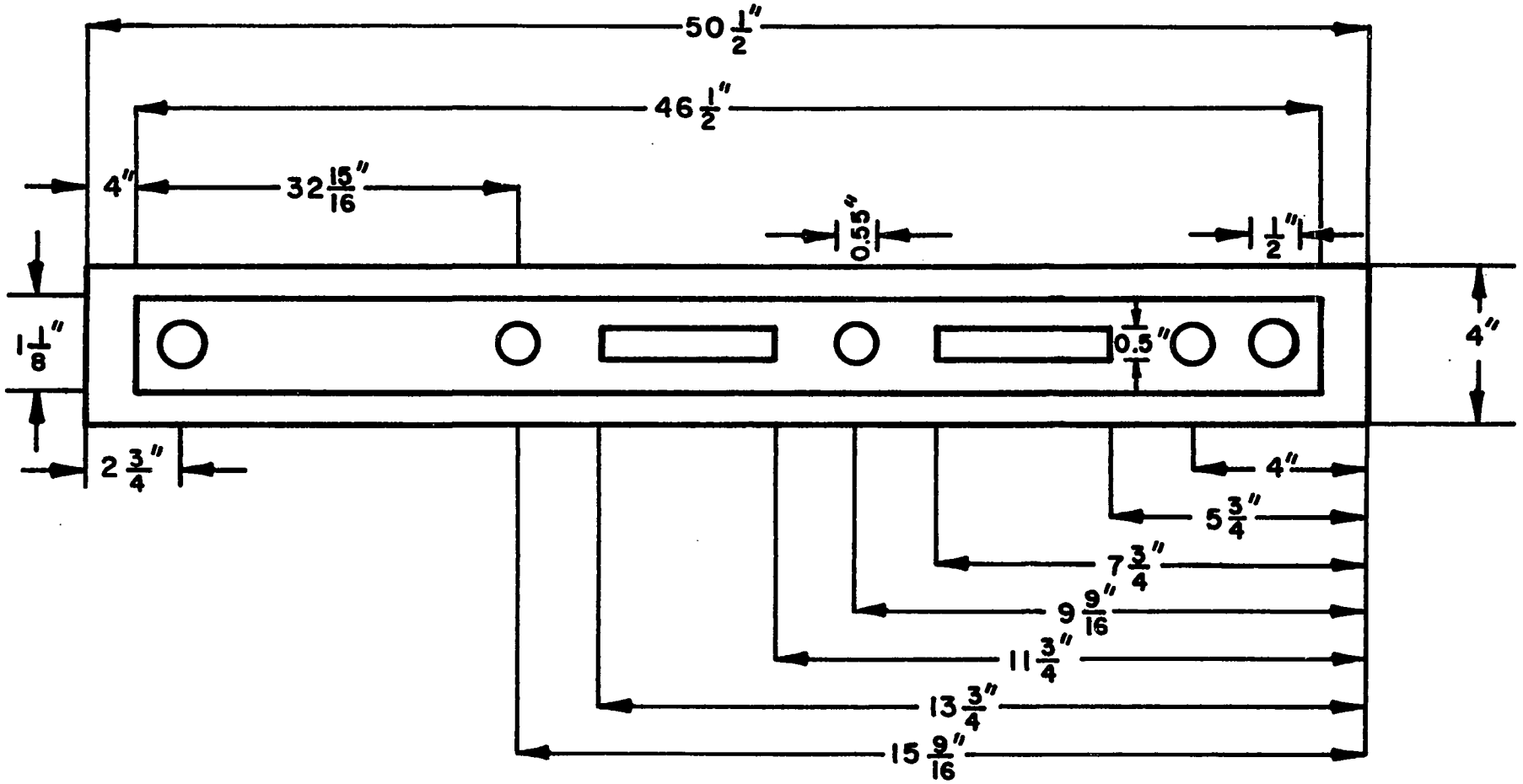

FIGURE 6. Dimensions of bottom sheet of the flow cell. (Not to scale)

the center of the test section. The first hole was at the entrance of the test section. The distance between two consecutive holes was 0.4 in., center to center. Thirty working glassy carbon disc electrodes were mounted in the holes of the cover sheet and smoothed flush with the inner surface of the cover sheet. The working disc electrode installed at the entrance of the test section was #1 and the one at the end of the test section was #30. The details of the cover sheet are shown in Figure 7.

Finally, the two plexiglas sheets were bolted together. A rubber gasket of 0.02 in. (type Buna/N, Industrial Gasket Inc., Oklahoma City, OK 73124) was used to seal the two plexiglas sheets. The flow cell was mounted horizontally and a portion of the plastic tubes of the working electrodes were filled with mercury and a 16-gauge wire was dipped in each tube for electrical contact between the carbon electrode and the external circuit. Figure 8 shows one of these glassy carbon electrodes mounted in the flow cell.

Procedure

All buffer solutions were prepared from sodium phosphate. From preliminary tests and from the studies cited in[80-83], it was found that a suitable applied voltage range was -0.1 to +0.7. It has also been

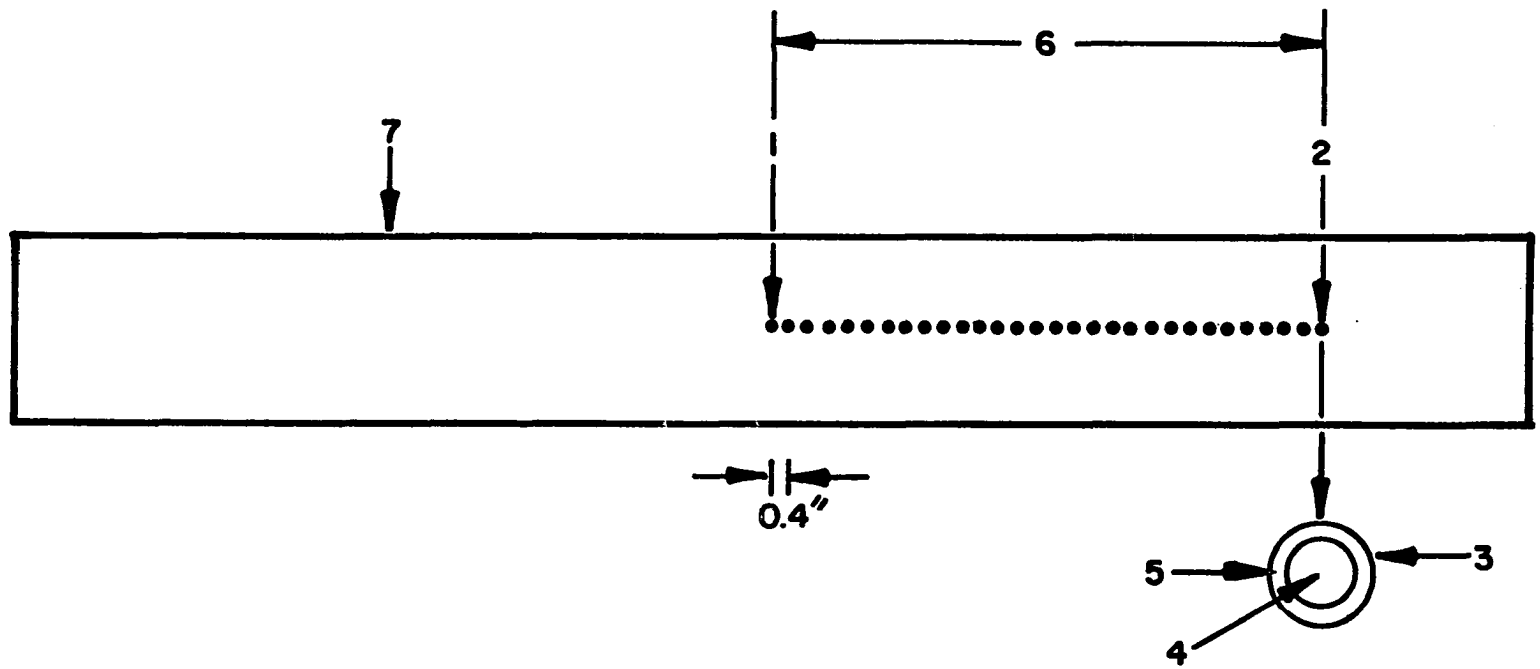

FIGURE 7. Details of cover sheet of flow cell. (1) glassy carbon working electrode no. 1. (2) glassy carbon working electrode no. 30. (3) plastic tube. (4) 3 mm glassy carbon disc. (5) epoxy adhesive. (6) test section in cover sheet. (7) cover sheet of flow cell.

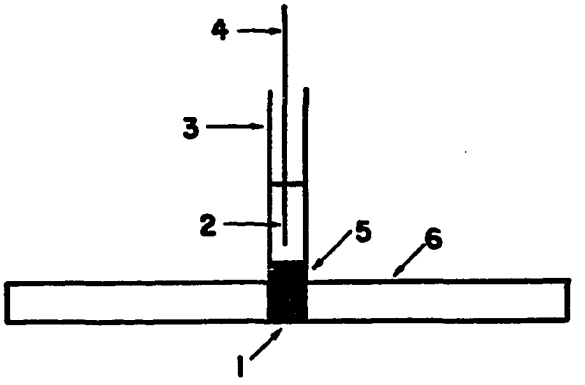

FIGURE 8. Details of glassy carbon working disc electrode mounted in the cover sheet of the flow cell. (1) 3 mm dia. glassy carbon disc. (2) mercury pool for electrical contact. (3) plastic tube. (4) 16-gauge copper wire. (5) 2cm x .3cm dia. glassy carbon rod. (6) cover sheet of the flow cell.

reported that the adsorbed NAD^+ was reduced, and desorbed at a potential more negative than -1.3 V. In our study, a cyclic potential of ± 1.4 V is used to condition and pretreat the electrodes with the procedure described by Blaedel and Jenkins[80,81] which follows:

Electrode Conditioning. The glassy working disc electrodes are conditioned and pretreated following the Blaedel and Jenkins procedure[80,81]. The conditioning of the electrodes involves first deaerating the buffer solution in the flow system and then applying an anodic potential of 1.4 V for two minutes and then a cathodic potential of -1.4 for two minutes for each working electrode. Conditioning consisted of 15 such cycles. It was carried out only once in the past history of the electrode.

Electrode Pretreatment. Pretreatment involves applying two cycles only. It was done before each new single experiment to clean the electrode surface of any surface functional groups. Conditioning and pretreatment are accomplished by using both the circuit shown in Figures 1 and 2 and the PAR, Figure 9.

Prior to the start of each experiment, nitrogen gas was bubbled into the storage tank for one hour before any new experiment to remove dissolved oxygen to avoid

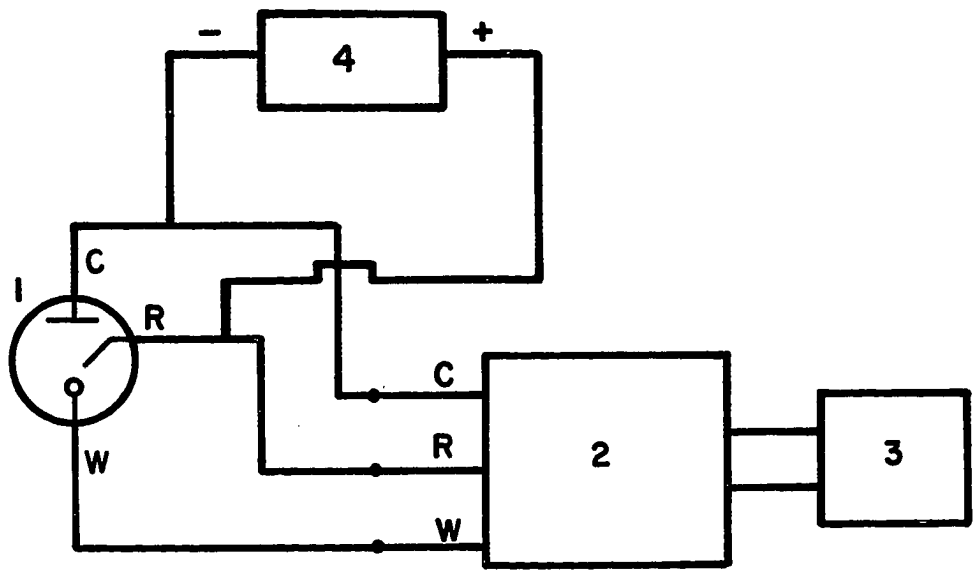

FIGURE 9. Electric circuit for 3-electrode system using scanning technique. (1) flow cell. (2) polarographic analyzer. (3) x-y recorder. (4) digital voltmeter. (C) platinum counter current electrode. (R) Ag/AgCl reference electrode. (W) glassy carbon electrode.

all interference with the current-voltage data. A stream of nitrogen gas was also passed over the test solution in the storage tank during the whole experiment. The flow system was kept at a constant temperature of 26°C (± 0.1°C).

Following pretreatment, the SSV method and the scanning method were used to obtain current-potential curves (voltammograms) at the applied potential range of -0.1V to +0.7V. The Re values of 7174, 10782, 14307 and 24882 are used to get voltammograms for one electrode only (#5). The electrode is held at 0 V for about 30 minutes before each voltammogram so the background current can return to its normal state, that is within a few nanoamperes of the fresh background current[80,83]. After the background voltammogram determination, a fresh stock solution of NADH/NAD^+ was added to the buffer to bring the test solution to 10 μM in NADH and 20 μM in NAD^+. Then voltammograms for NADH/NAD^+ solution were obtained at the same conditions and same flow rates using the same procedure as used for the background current determination.

With the SSV method, the 2-electrode setup, Figure 1, and 3-electrode setup, Figure 2 and Figure 9 were used to obtain voltammograms, pointwise in increments of 20 mv. The initial voltage (-0.1V) was applied first between the working electrode and the reference

electrode. When the resultant current reached its steady state value, this value was recorded. The applied voltage was increased by an increment of 20 mv and the procedure repeated for recording the steady state current. The voltage was increased and the above procedure repeated until we reached 0.7V.

With the scanning method, only the 3-electrode set-up, Figure 9 was used to obtain continuous voltammograms. The initial potential was set at -0.1V by the initial potential controls on the PAR. The digital voltmeter was used to monitor the initial potential. The polarity control of the initial potential on the PAR was set on negative. The scan rate was set to 5 mv/sec. The direction of the scan was positive. The voltage range control was set at 3V, and the current range control was set at 5 μA (this gives a 0.5 μA/in on the "x-y" recorder since the full scale "Y" axis is 10V). These procedures were chosen, so that the scan begins at -0.1V and automatically advances to 2.9V, but scanning was manually terminated at 0.7V. $NADH/NAD^+$ stock solution was added after reproducible background voltammograms were obtained and after the electrode was held at 0 V. Three voltammograms were obtained for each Re with the scanning method. A fresh $NADH/NAD^+$ solution was used to obtain each voltammogram.

To evaluate the performance of the flow system, voltammograms at the three values of Re for electrodes numbers 1, 10, 15, 20, 25, and 30 were also recorded by scanning, following the same procedure described above.

CHAPTER V

RESULTS AND DISCUSSION

Voltammograms

Figures 10 and 11 are voltammograms obtained by the SSV with the 2-electrode set-up and 3-electrode set-up at the glassy carbon disc electrode #5 for Re = 7174. Curve A is the background voltammetric curve, curve B is the NADH voltammetric curve and curve C is voltammetric curve B corrected for the background. Curve C indicates a very well-defined transport region (plateau). The limiting current value (I_L) obtained with the 2-electrode system (Figure 10, curve C) is 0.404 μA. The limiting current value (I_L) obtained with the 3-electrode system (Figure 11, curve C) is 0.37 μA. The agreement between these two values is within 8.4%. Both electrode set-ups are compatible. The 2-electrode set-up avoids using a counter electrode inside the flow cell which might disturb the flow and enhance the mass transfer. However, to avoid the problem of drawing current through the reference electrode, and to measure the true electrode potential, the 3-electrode set-up was used in all our experiments.

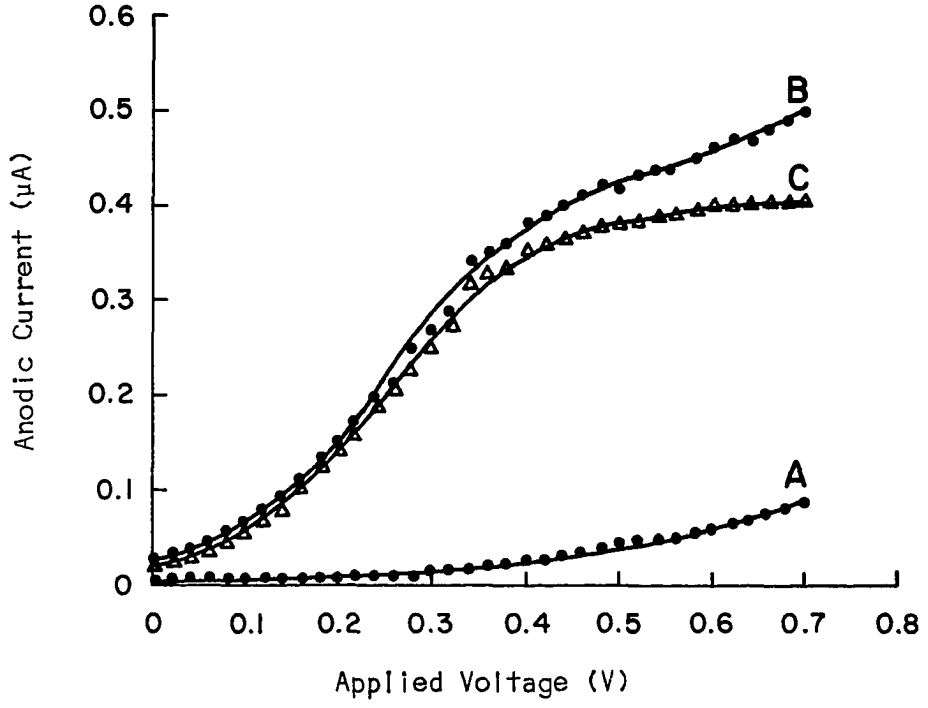

FIGURE 10. Voltammetric curves by SSV at glassy carbon disc electrode no. 5. Conditions: 10μM/NADH/20μM NAD^+ in 0.05M phosphate buffer, pH 9.2. Re = 7174. 2-electrode set-up. (A) Background, (B) 10μM NADH, (C) Curve B corrected for background current.

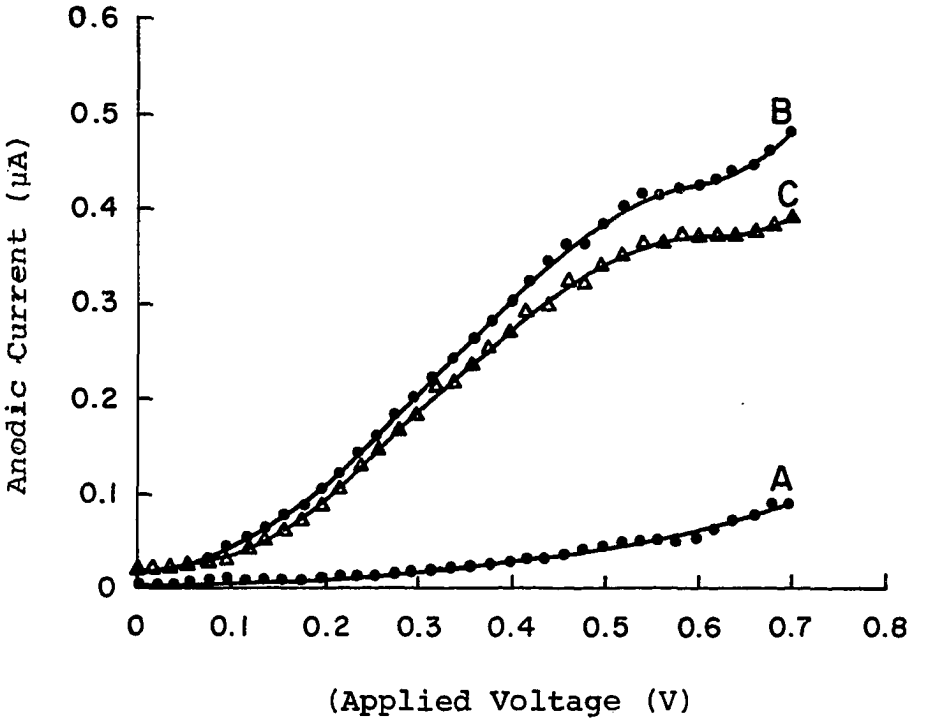

FIGURE 11. Voltammetric curves by SSV at glassy carbon disc electrode no. 5. Conditions: 10μM NADH/ 20μM NAD^+ in 0.05M phosphate buffer, pH 9.2. Re = 7174. 3-electrode set-up. (A) Background, (B) 10μM NADH, (C) Curve B corrected for background.

Figures 12, 13 and 14 are voltammograms obtained by SSV at disc electrode #5 for Re = 10782, 14307 and 2482 respectively. Curve C in these figures is curve B corrected for the background. Curve C in these figures indicates a very well-defined transport region. At the high value of Re = 24882, we faced a mechanical problem with the platinum sheet counter electrode located downstream of disc electrode #5. The platinum sheet was bent several times due to this high flow rate. Therefore, it was decided to use only the other smaller values of Re = 7174, 10782, and 14307.

The limiting current values obtained by SSV of Figures 11, 12, 13, and 14 are listed in Table 1 which shows that as the value of Re increases, the limiting current increases. These results are in agreement with the studies of Blaedel and Jenkins[81] with a glassy-carbon rotating disc electrode.

Although the SSV method produces well-defined voltammograms, it requires about 10 hours to obtain just one voltammogram for only one electrode for our flow system. It is clear that this is a tedious and time consuming task to carry out for the rest of the electrodes. In addition, too much fluctuation in the current reading was observed with the SSV. Therefore, we switched to the automatic scanning method which is a fast and easy data-taking technique. Besides, the scanning method had

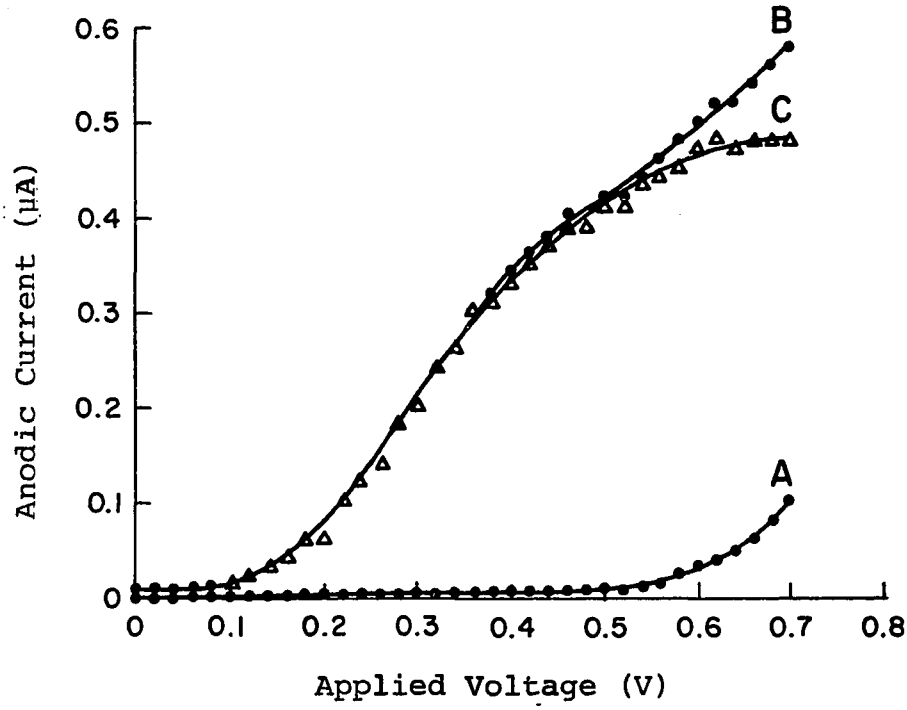

FIGURE 12. Voltammetric curve by SSV at glassy carbon disc electrode no. 5. Conditions: 10μM NADH/20μM NAD^+ in 0.05M phosphate buffer, pH 9.2. Re = 10782. (A) Background, (B) 10μM NADH, (C) Curve B corrected for background.

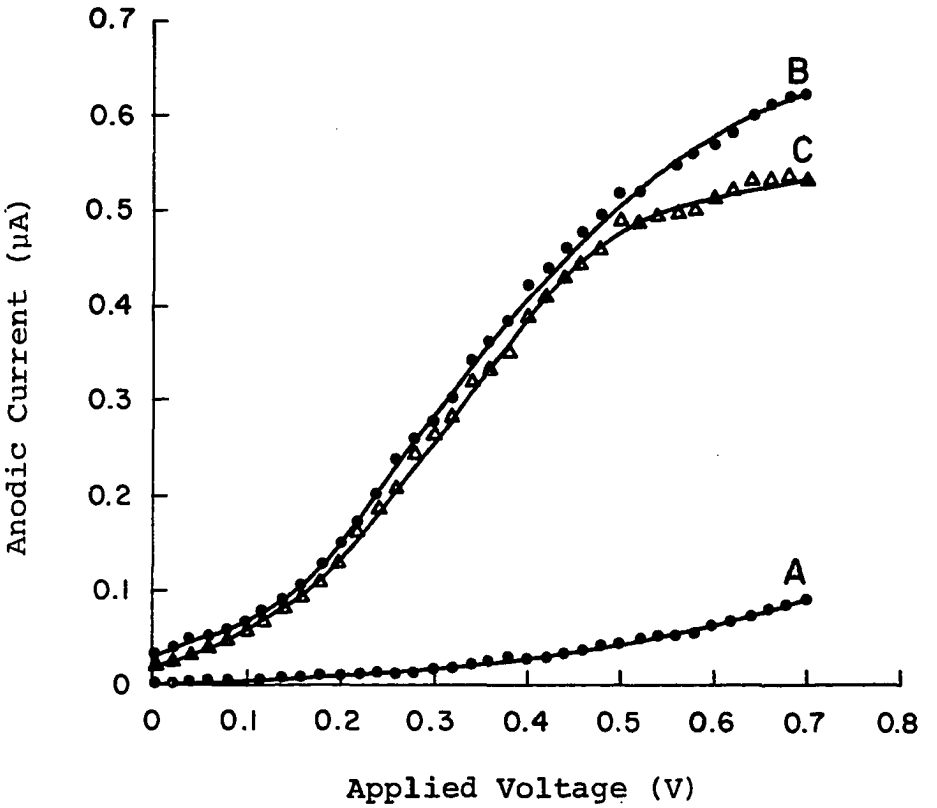

FIGURE 13. Voltammetric curves by SSV at glassy carbon disc electrode no. 5. Conditions: 10μM NADH/20μM NAD^+ in 0.05M phosphate buffer, pH 9.2. Re = 14307. 3-electrode set-up. (A) Background, (B) 10μM NADH, (C) Curve B corrected for background.

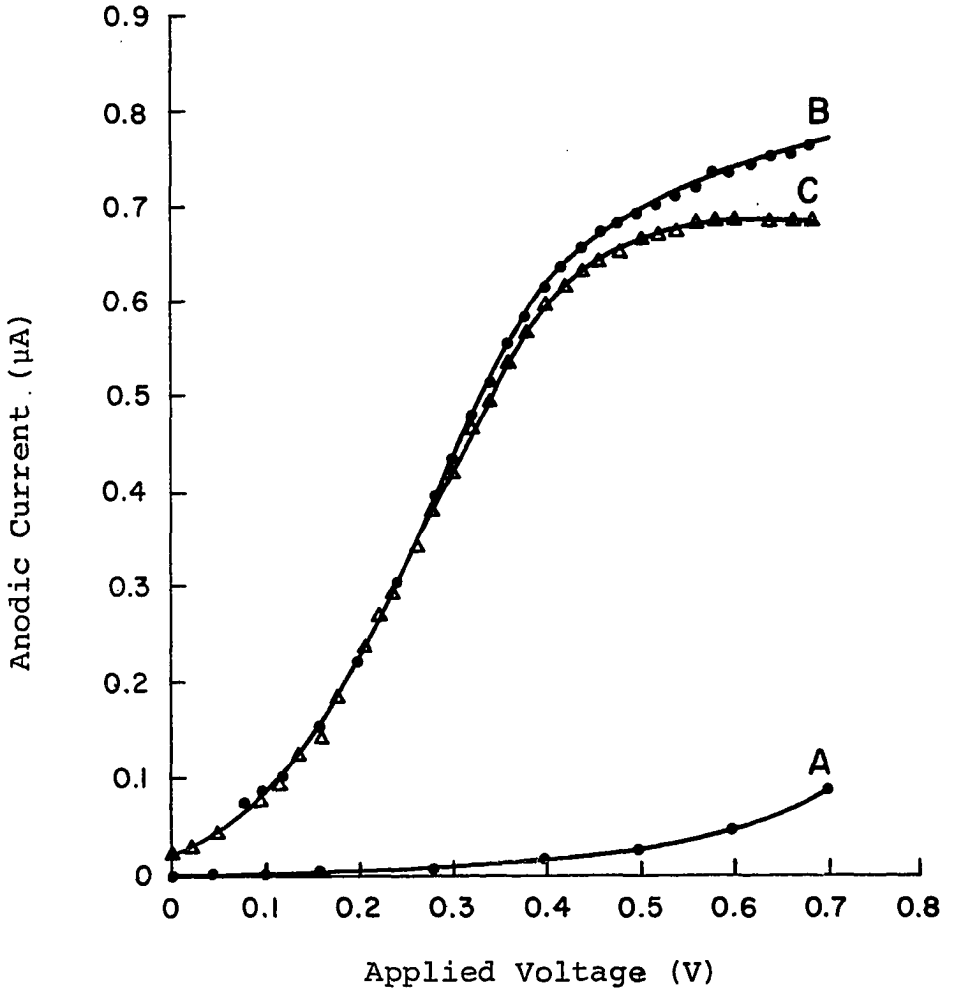

FIGURE 14. Voltammetric curves by SSV at glassy carbon disc electrode no. 5. Conditions: 10μM NADH/20μM NAD^+ in 0.1M phosphate buffer, pH 7.7. Re = 24882. 3-electrode set-up. (A) Background, (B) 10μM NADH, (C) Curve B corrected for background.

TABLE 1

LIMITING CURRENT VALUES (I_L) OBTAINED BY SSV

AT GLASSY CARBON DISC ELECTRODE #5

Re	I_L(μA)	Figure
7174	0.37	11
10782	0.48	12
14307	0.53	13
24882	0.69	14

been successfully used by Moiroux and Elving[82,83] with the NADH system. The technique involves using the PAR with the x-y recorder to record voltammetric curves (at a certain voltage range, selected scan rate, and selected current sensitivity) for the background and the NADH/NAD^+ solution. The NADH curves have to be corrected for the background to get the true limiting current value (I_L). For our flow system, we used a voltage range of -0.1 V to + 0.7 V, and a scan rate of 5 mv/sec. Figures 15 to 21 are voltammograms recorded by scanning at Re = 7174 for 10 μM NADH + 20 μM NAD^+ in 0.05M phosphate buffer, pH 9.2 at glassy carbon disc electrodes numbers 1, 5, 10, 15, 20, 25 and 30.

Figures 22 to 28 are voltammograms recorded by scanning at Re = 10782 for the same disc electrodes under the same conditions as Figures 15 to 21.

Figures 29 to 35 are voltammograms recorded by scanning at Re = 14307 for the same disc electrodes and under the same conditions as Figures 15 to 21.

In the aforementioned figures, curve A is the background voltammetric curve, curve B is the NADH curve and curve C is curve B corrected for the background which indicates a very well-defined transport region (plateau).

Figure 36 shows the three plateaus (voltammetric curves) obtained at the three values of Re = 7174, 10782,

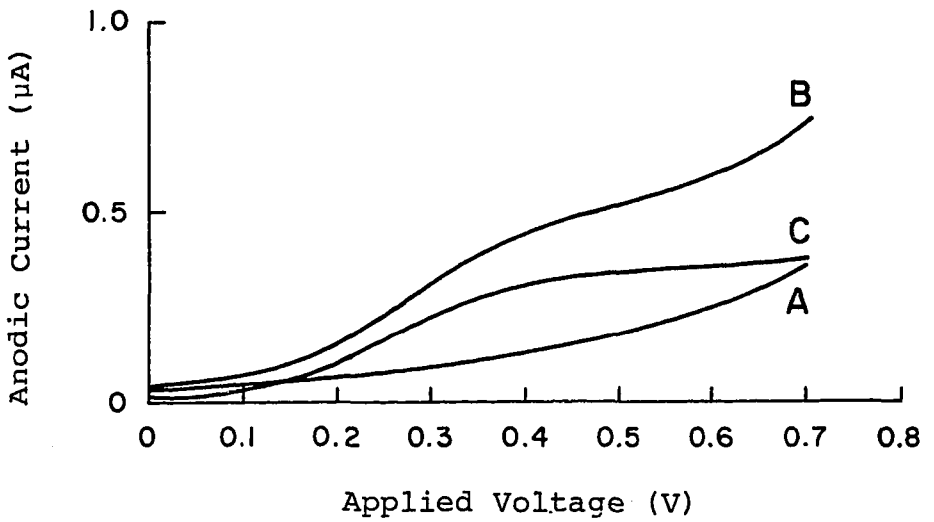

FIGURE 15. Voltammetric curves by scanning at glassy carbon disc electrode no. 1. Conditions: 10μM NADH/20μM NAD^+ in 0.05M phosphate buffer, pH 9.2. Re = 7174. (A) Background, (B) 10μM NADH, (C) Curve B corrected for background.

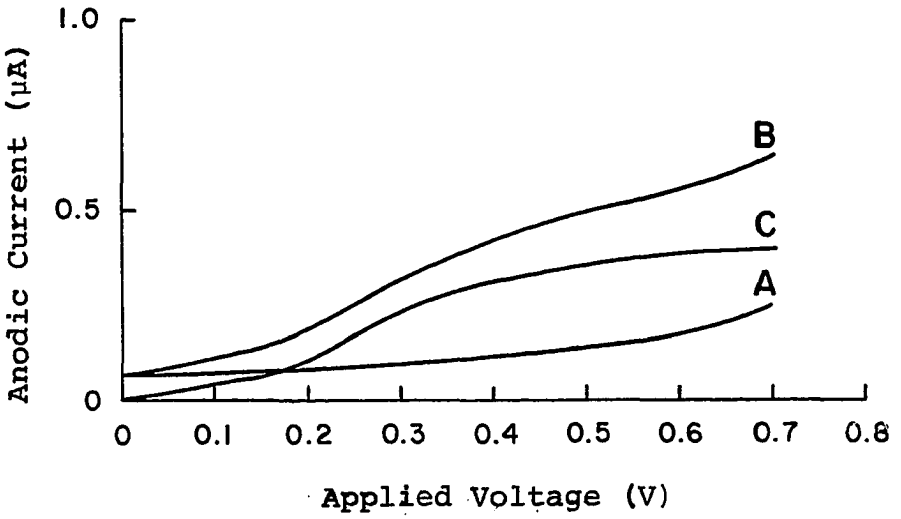

FIGURE 16. Voltammetric curves by scanning at glassy carbon disc electrode no. 5. Conditions: 10μM NADH/ 20μM NAD^+ in 0.05M phosphate buffer, pH 9.2. Re = 7174. (A) Background, (B) 10μM NADH, (C) Curve B is corrected for background.

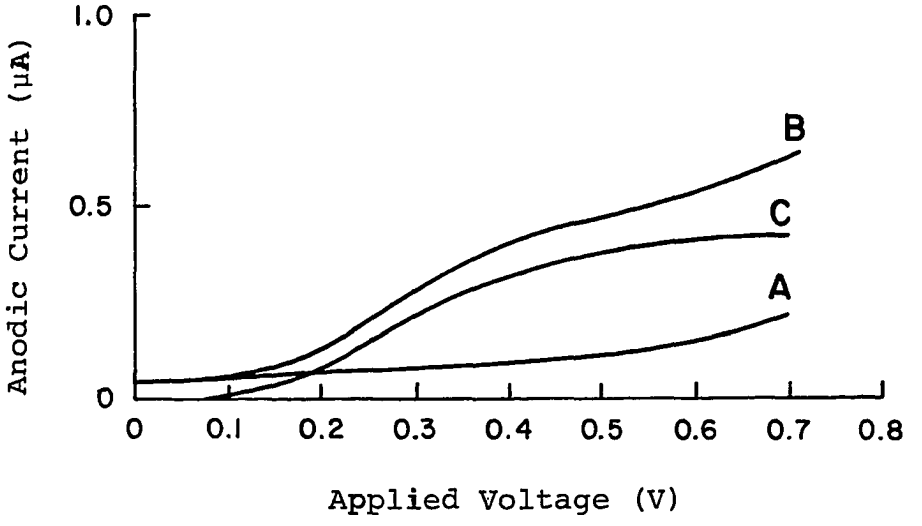

FIGURE 17. Voltammetric curves by scanning at glassy carbon disc electrode no. 10. Conditions: 10μM NADH/ 20μM NAD^+ in 0.05M phosphate buffer, pH 9.2. Re = 7174. (A) Background, (B) 10μM NADH, (C) Curve B corrected for background.

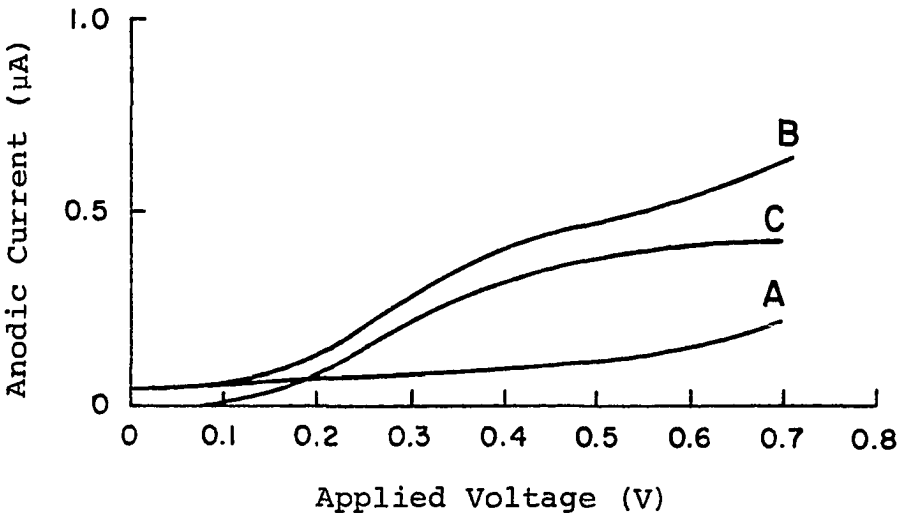

FIGURE 18. Voltammetric curves by scanning at glassy carbon disc electrode no. 15. Conditions: 10μM NADH/ 20μM NAD^+ in 0.05M phosphate buffer, pH 9.2. Re = 7174. (A) Background, (B) 10μM NADH, (C) Curve B corrected for background.

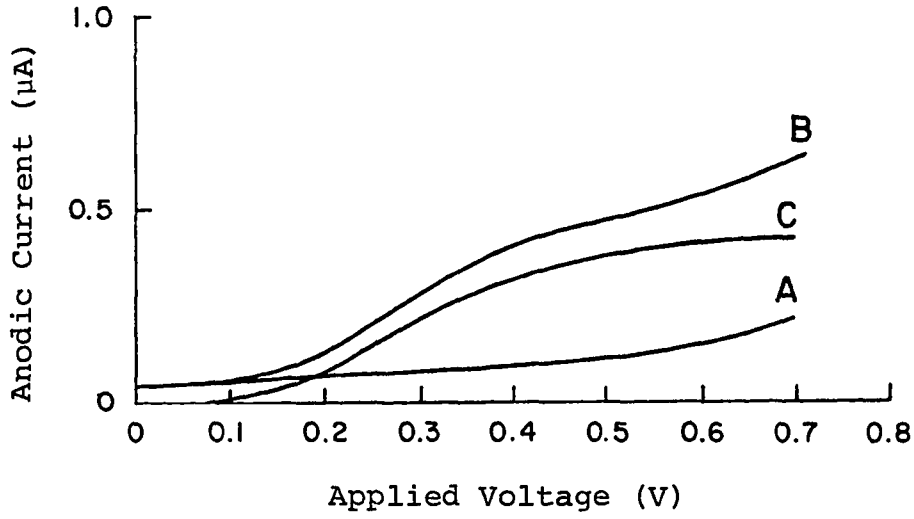

FIGURE 19. Voltammetric curves by scanning at glassy carbon disc electrode no. 20. Conditions: 10μM NADH/ 20μM NAD^+ in 0.05M phosphate buffer, pH 9.2. Re = 7174. (A) Background, (B) 10μM NADH, (C) Curve B corrected for background.

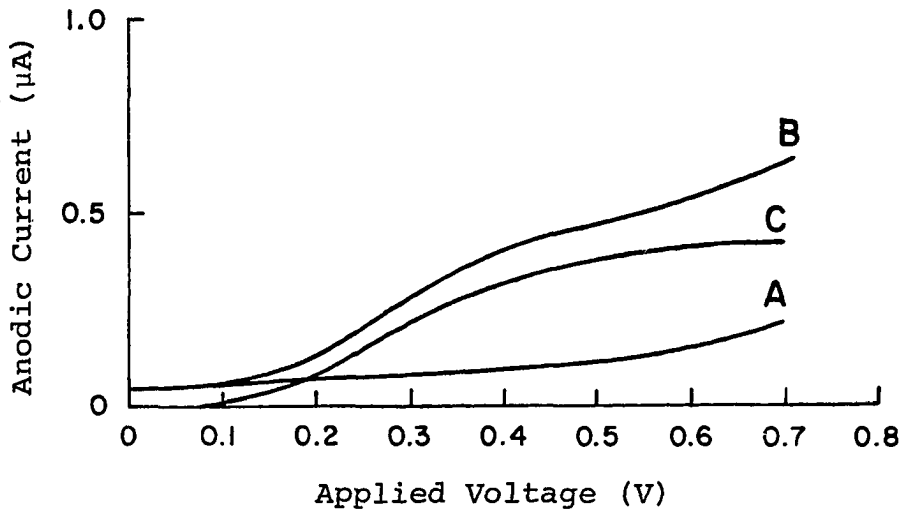

FIGURE 20. Voltammetric curves by scanning at glassy carbon disc electrode no. 25. Conditions: 10μM NADH/ 20μM NAD^+ in 0.05M phosphate buffer, pH 9.2. Re = 7174. (A) Background, (B) 10μM NADH, (C) Curve B corrected for background.

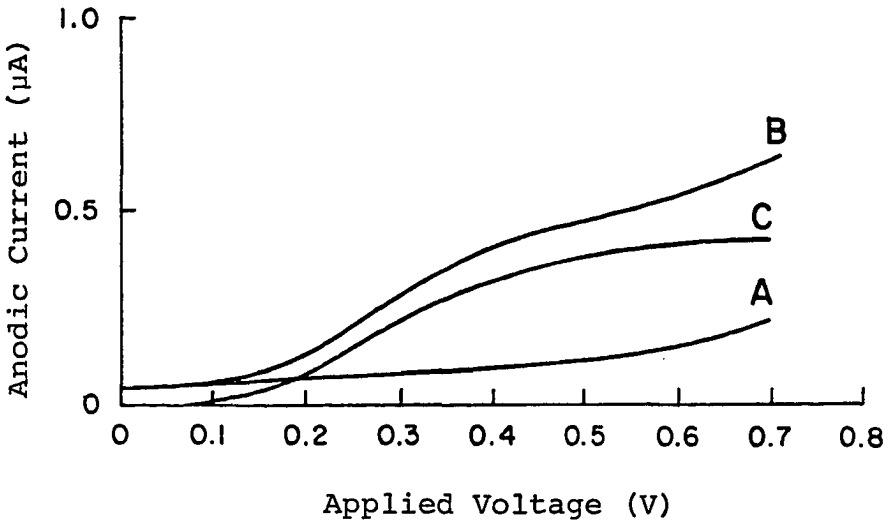

FIGURE 21. Voltammetric curves by scanning at glassy carbon disc electrode no. 30. Conditions: 10μM NADH/ 20μM NAD^+ in 0.05M phosphate buffer, pH 9.2. Re = 7174. (A) Background, (B) 10μM NADH, (C) Curve B corrected for background.

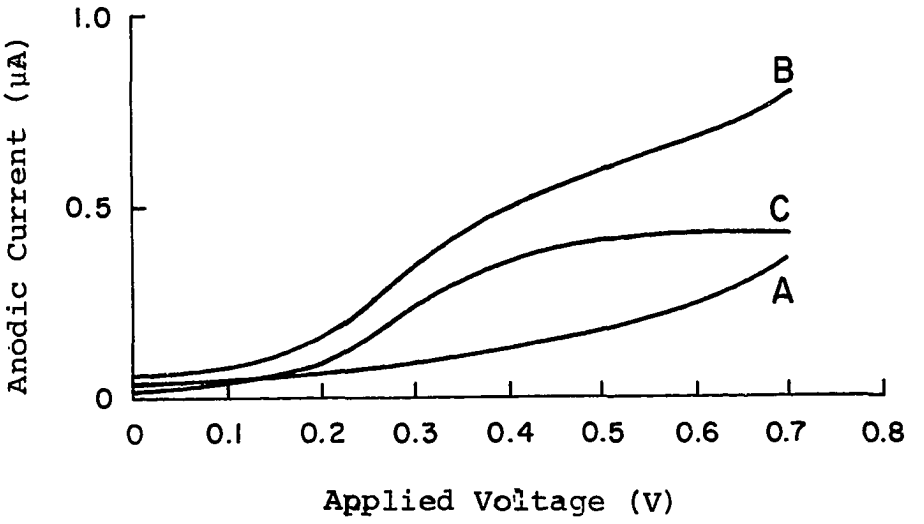

FIGURE 22. Voltammetric curves by scanning at glassy carbon disc electrode no. 1. Conditions: 10μM NADH/ 20μM NAD^+ in 0.05M phosphate buffer, pH 9.2. Re = 10782. (A) Background, (B) 10μM NADH, (C) Curve B corrected for background.

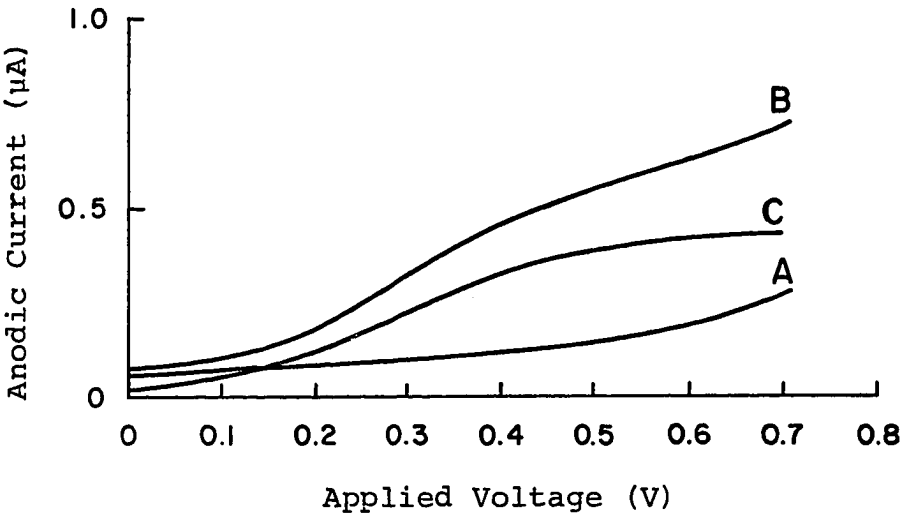

FIGURE 23. Voltammetric curves by scanning at glassy carbon disc electrode no. 5. Conditions: 10μM NADH/ 20μM NAD^+ in 0.05M phosphate buffer, pH 9.2. Re = 10782. (A) Background, (B) 10μM NADH, (C) Curve B corrected for background.

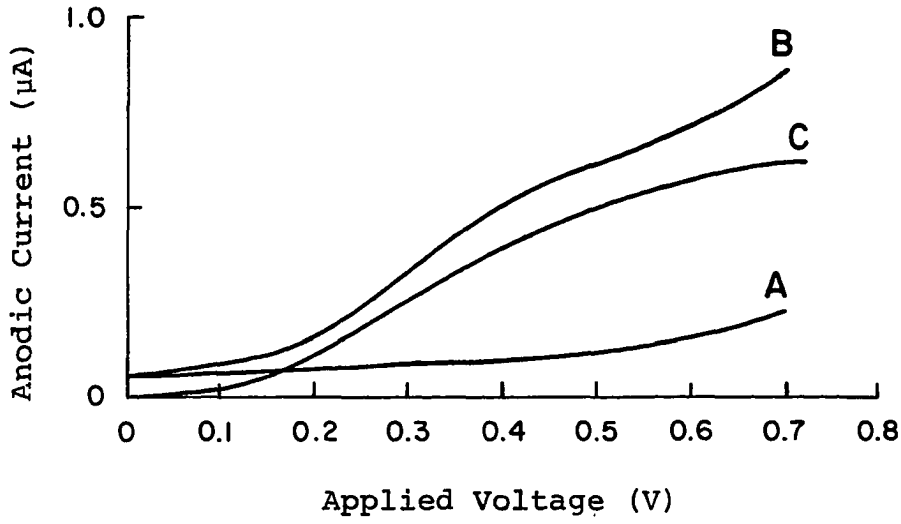

FIGURE 24. Voltammetric curves by scanning at glassy carbon disc electrode no. 10. Conditions: 10μM NADH/ 20μM NAD^+ in 0.05M phosphate buffer, pH 9.2. Re = 10782. (A) Background, (B) 10μM NADH, (C) Curve B corrected for background.

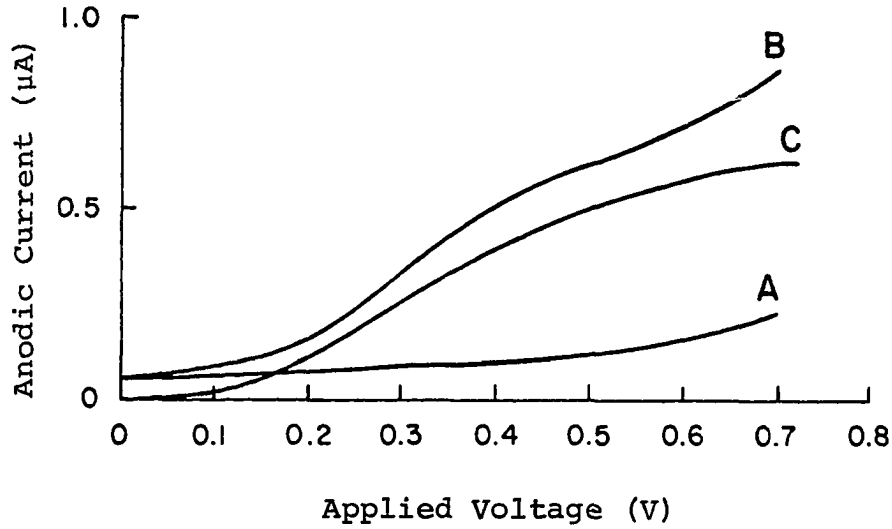

FIGURE 25. Voltammetric curves by scanning at glassy carbon disc electrode no. 15. Conditions: 10μM NADH/ 20μM NAD^+ in 0.05M phosphate buffer, pH 9.2. Re = 10782. (A) Background, (B) 10μM NADH, (C) Curve B corrected for background.

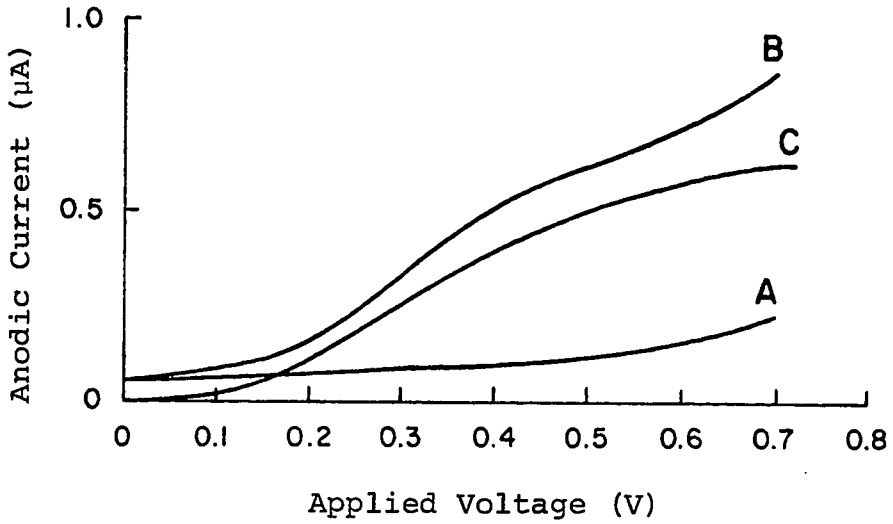

FIGURE 26. Voltammetric curves by scanning at glassy carbon disc electrode no. 20. Conditions: 10μM NADH/ 20μM NAD^+ in 0.05M phosphate buffer, pH 9.2. Re = 10782. (A) Background, (B) 10μM NADH, (C) Curve B corrected for background.

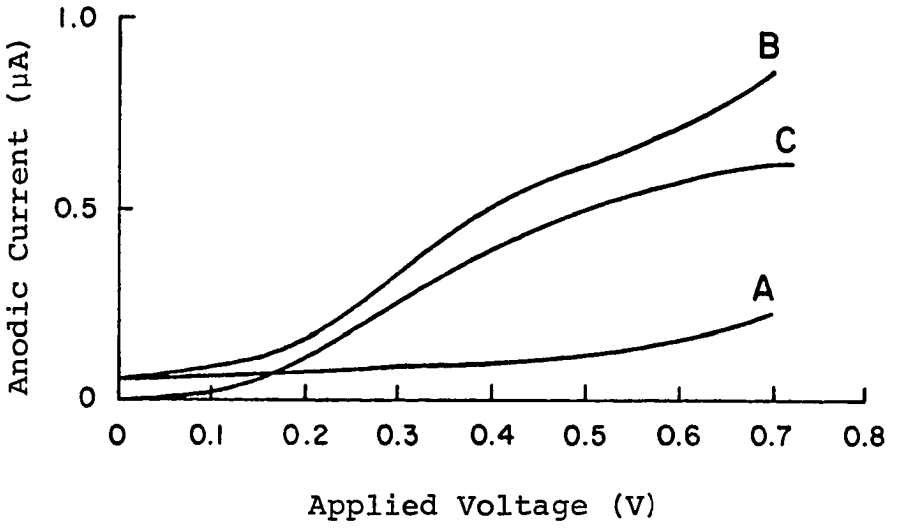

FIGURE 27. Voltammetric curves by scanning at glassy carbon disc electrode no. 25. Conditions: 10μM NADH/ 20μM NAD^+ in 0.05M phosphate buffer, pH 9.2. Re = 10782. (A) Background, (B) 10μM NADH, (C) Curve B corrected for background.

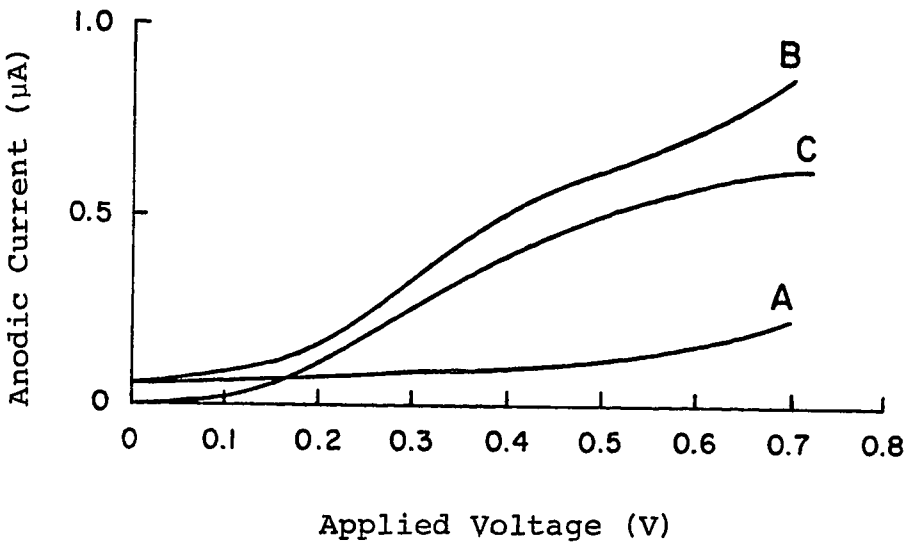

FIGURE 28. Voltammetric curves by scanning at glassy carbon disc electrode no. 30. Conditions: 10μM NADH/ 20μM NAD^+ in 0.05M phosphate buffer, pH 9.2. Re = 10782. (A) Background, (B) 10μM NADH, (C) Curve B corrected for background.

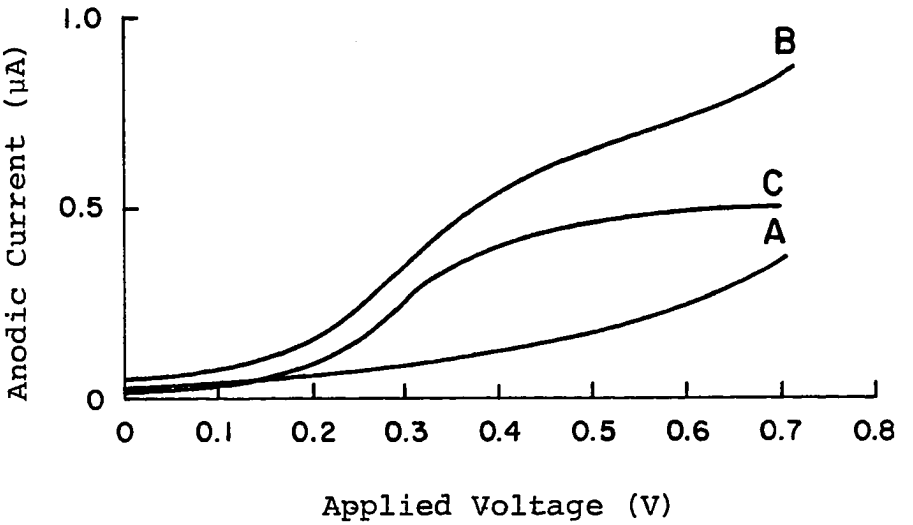

FIGURE 29. Voltammetric curves by scanning at glassy carbon disc electrode no. 1. Conditions: 10μM NADH/ 20μM NAD^+ in 0.05M phosphate buffer, pH 9.2. Re = 14307. (A) Background, (B) 10μM NADH, (C) Curve B corrected for the background.

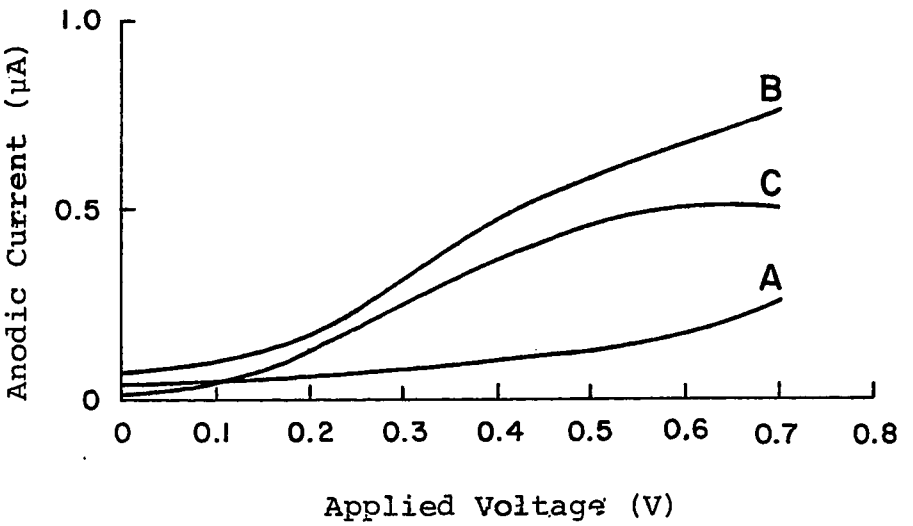

FIGURE 30. Voltammetric curves by scanning at glassy carbon disc electrode no. 5. Conditions: 10μM NADH/ 20μM NAD^+ in 0.05M phosphate buffer, pH 9.2. Re = 14307. (A) Background, (B) 10μM NADH, (C) Curve B corrected for background.

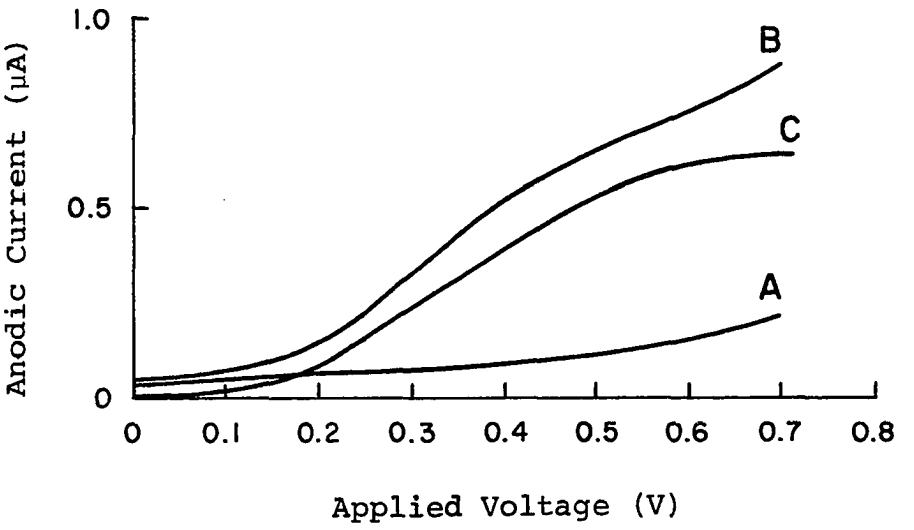

FIGURE 31. Voltammetric curves by scanning at glassy carbon disc electrode no. 10. Conditions: 10μM NADH/ 20μM NAD^+ in 0.05M phosphate buffer, pH 9.2. Re = 14307. (A) Background, (B) 10μM NADH, (C) Curve B corrected for background.

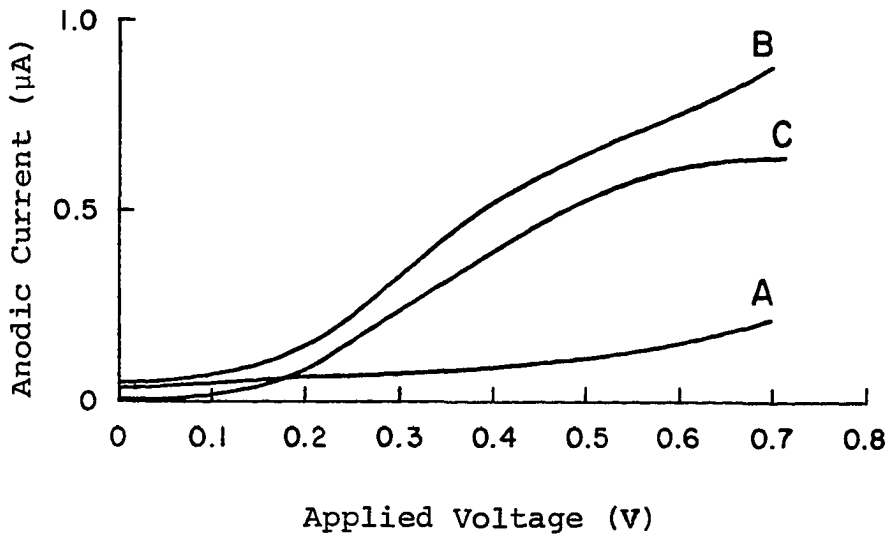

FIGURE 32. Voltammetric curves by scanning at glassy carbon disc electrode no. 15. Conditions: 10μM NADH/ 20μM NAD^+ in 0.05M phosphate buffer, pH 9.2. Re = 14307. (A) Background, (B) 10μM NADH, (C) Curve B corrected for background.

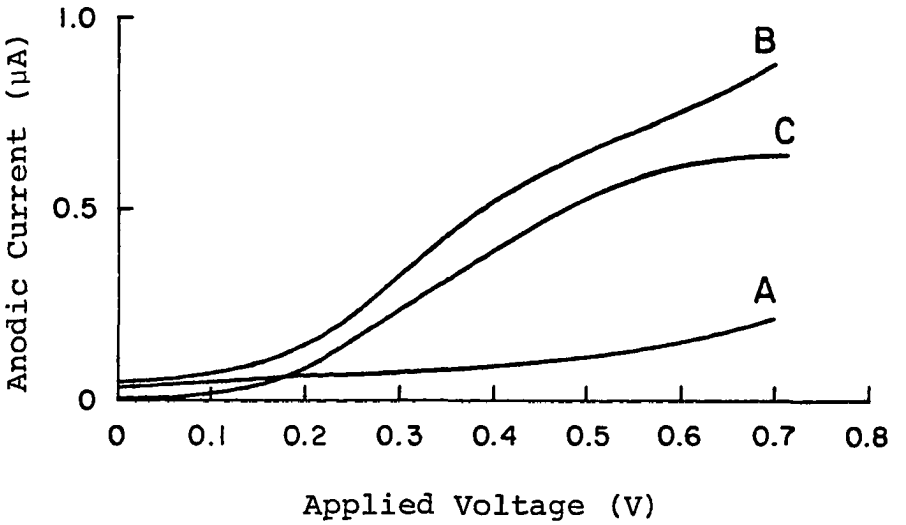

FIGURE 33. Voltammetric curves by scanning at glassy carbon disc electrode no. 20. Conditions: 10μM NADH/ 20μM NAD^+ in 0.05M phosphate buffer, pH 9.2. Re = 14307. (A) Background, (B) 10μM NADH, (C) Curve B corrected for background.

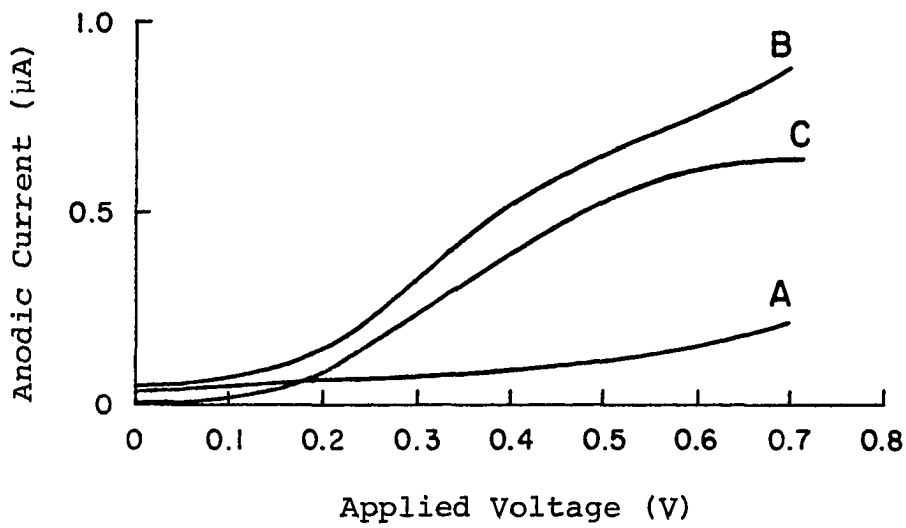

FIGURE 34. Voltammetric curves by scanning at glassy carbon disc electrode no. 25. Conditions: 10μM NADH/ 20μM NAD^+ in 0.05M phosphate buffer, pH 9.2. Re = 14307. (A) Background, (B) 10μM NADH, (C) Curve B corrected for background.

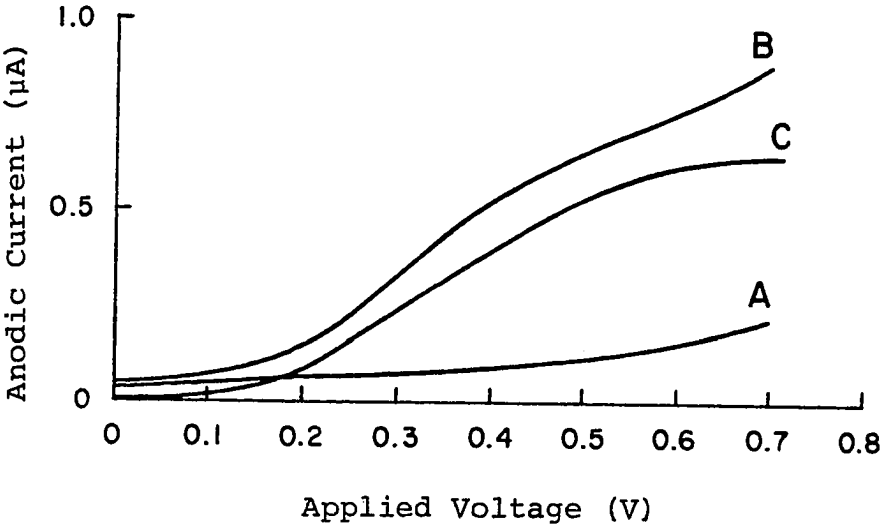

FIGURE 35. Voltammetric curves by scanning at glassy carbon disc electrode no. 30. Conditions: 10μM NADH/ 20μM NAD^+ in 0.05M phosphate buffer, pH 9.2. Re = 14307. (A) Background, (B) 10μM NADH, (C) Curve B corrected for background.

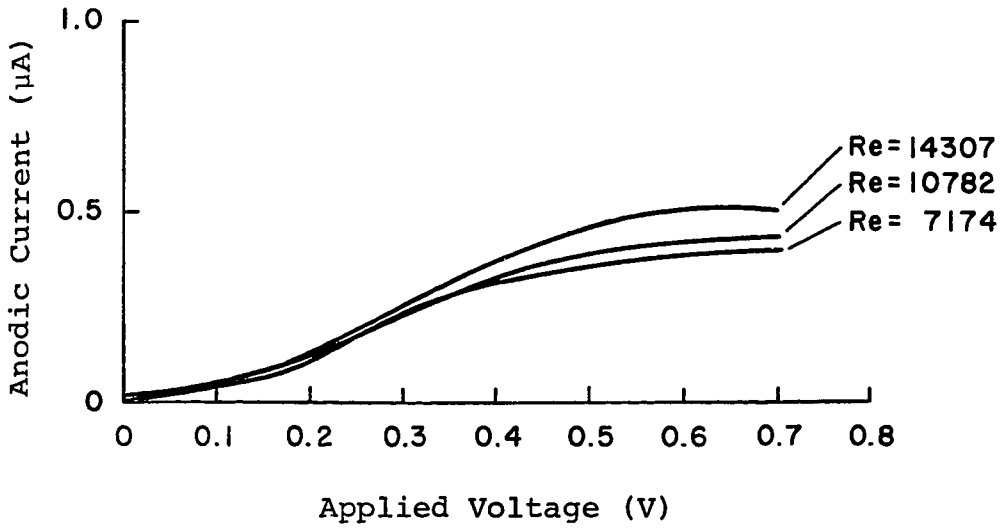

FIGURE 36. Combined voltammetric curves at Re = 7174, 10782, and 14307 for glassy carbon disc electrode #5.

and 14307 for the glassy-carbon disc electrode #5 in our flow cell. These three plateaus are the plateaus (curve C) of Figures 16, 23, and 30. They have been combined just to compare our results to the literature. Figure 36 shows voltammograms which are qualitatively similar to the ones obtained by Blaedel and Jenkins[81].

To our knowledge, no study has been reported in the literature of the electrochemical oxidation of NADH nor any other macromolecular system in flow cells which produced well-defined plateaus similar to the ones shown in Figures 15 to 35. The studies by Blaedel and Jenkins[80,81] and by Moiroux and Elving[82,83] are for the electrochemical oxidation of NADH at rotating, or stationary glassy carbon disc electrodes in H-type cells or in three compartment cells. In these studies[80-83] well-defined voltammograms were obtained at different rotations per minute (RPM). These studies were designed to determine the NADH concentrations at micromolar levels or to detect the presence of impurities by their reaction with NAD^+ to produce NADH.

The limiting current values taken from curve C of the above figures are listed in Tables 2, 3 and 4. These tables show that the limiting current values at electrode #'s 1 and 5 are lower than the limiting current values of the following electrodes. Since the entry effects were eliminated by preceding the test section by

TABLE 2

LIMITING CURRENT VALUES OBTAINED BY SCANNING

AT Re = 7174

Elect. No.	I_L (μA)	Figure
1	0.40	15
5	0.40	16
10	0.43	17
15	0.43	18
20	0.43	19
25	0.43	20
30	0.43	21

TABLE 3

LIMITING CURRENT VALUES OBTAINED BY SCANNING

AT Re = 10782

Elect. No.	I_L (μA)	Figure
1	0.43	22
5	0.43	23
10	0.61	24
15	0.61	25
20	0.61	26
25	0.61	27
30	0.61	28

TABLE 4

LIMITING CURRENT VALUES OBTAINED BY SCANNING

AT Re = 14307

Elect. No.	I_L (μA)	Figure
1	0.50	29
5	0.51	30
10	0.63	31
15	0.63	32
20	0.63	33
25	0.63	34
30	0.63	35

a length of about 80 diameter[65,90], and since the adsorption problem has been compensated for by adding excess amounts of NAD^+[82,83], possible interpretations for this phenomena are: 1) the platinum sheet counter electrode located downstream of electrode #5 disturbed the flow pattern and increased the effective Re, 2) there could be small variation in the dimension of the flow cell along the length of the channel in this region. These factors could have enhanced the mass transfer rates for the downstream glassy carbon working disc electrodes numbers 6 to 30, i.e. This would increase the limiting current value for electrode number 6 and up. The investigation of this phenomenon is recommended for further study.

Assuming that the limiting current values obtained at electrode #5 represent the true value of the mass transfer, the values listed in Table 1 are compared with those listed in Tables 2, 3 and 4. Table 5 shows the percent of agreement among those values.

TABLE 5

PERCENT OF AGREEMENT BETWEEN THE SSV VALUES AND THE SCANNING ONES FOR ELECTRODE #5

Re	I_L (μA) by SSV	I_L (μA) by Scanning	% Agreement	Figure
7174	0.37	0.40	7.50	11,16
10782	0.48	0.43	10.40	12,23
14307	0.53	0.51	3.80	13,30

We can say that the limiting current values obtained by scanning is within 3.8 to 10.4% of those obtained with SSV.

Mass Transfer Coefficient

The experimental local mass transfer coefficient (k) was calculated from equation (6),

$$k = \frac{I_L}{nF\ A\ C_b} \qquad (6)$$

The area A in equation (6) is the effective area of the electrode surface. This area can be found by recording current-time decay curve under linear diffusion conditions for potassium ferrocyanide and using the Cottrell equation[84,91], or by measurement of the current peak of potassium ferrocyanide cyclic voltammetry and using Randles-Sevick equation[78,93]. It was found[92] that the first method is more practical to use. The effective area of one of our glassy carbon disc electrodes has been measured using the facilities in the chemistry department and utilizing the first method. The current-decay curve is shown in Figure 39 and the calculation of the effective area is shown in Appendix B. The effective area of our electrode is found to be 0.0789 cm^2. The geometrical area of this electrode (.3cm in diameter) is found to be 0.071 cm^2. Moiroux and Elving[82] have

used a 5 mm in diameter glassy carbon disc electrode. They have found the effective area to be 0.23 cm^2 compared to the geometrical area of 0.2 cm^2. This shows that the geometrical area is a very good estimate of the effective area especially for glassy carbon electrodes[93]. Therefore, the experimental local mass transfer coefficients using equation (6) with A = 0.0789 cm^2 were calculated for all the limiting current values listed in Tables 1 to 4. The results are shown in Tables 6 to 9. These tables indicate that as the flow rate increases the local mass transfer increases too. All these results shown in Tables 6 to 9 are consistent with the literature[65]. Tables 7 to 9 also indicate that the local mass transfer coefficient has been enhanced for electrodes numbers 10, 15, 20, 25, and 30. This enhancement is due to the mechanical problem previously mentioned concerning the platinum sheet counter electrode located downstream of electrode #5. A sample calculation of the experimental, local k's is given in Appendix C.

The local mass transfer coefficient was also calculated by equation (8) cited in reference (65),

$$St = \frac{k}{v} = 0.0165\ Re^{-.14}\ Sc^{-.67} \qquad (8)$$

where

$$Sc = \frac{\nu}{D} \qquad (9)$$

TABLE 6

LOCAL MASS TRANSFER COEFFICIENT (k) FOR LIMITING CURRENT VALUES (I_L) OBTAINED BY SSV AT DISC ELECTRODE #5

Re	I_L (μA)	$k \times 10^3$ (cm/sec)	Figure
7174	0.37	2.43	11
10782	0.48	3.15	12
14307	0.53	3.48	13
24882	0.69	4.53	14

TABLE 7

LOCAL MASS TRANSFER COEFFICIENT FOR LIMITING CURRENT VALUES (I_L) OBTAINED BY SCANNING AT Re = 7174

Elect. No.	I_L (μA)	$k \times 10^3$ (cm/sec)	Figure
1	0.40	2.63	15
5	0.40	2.63	16
10	0.43	2.83	17
15	0.43	2.83	18
20	0.43	2.83	19
25	0.43	2.83	20
30	0.43	2.83	21

TABLE 8

LOCAL MASS TRANSFER COEFFICIENT FOR LIMITING CURRENT VALUES (I_L) OBTAINED BY SCANNING AT Re = 10782

Elec. No.	I_L (μA)	$k \times 10^3$ (cm/sec)	Figure
1	0.43	2.83	22
5	0.43	2.83	23
10	0.61	4.00	24
15	0.61	4.00	25
20	0.61	4.00	26
25	0.61	4.00	27
30	0.61	4.00	28

TABLE 9

LOCAL MASS TRANSFER COEFFICIENT FOR LIMITING CURRENT VALUES OBTAINED BY SCANNING AT Re = 14307

Elec. No.	I_L (μA)	$k \times 10^3$ (cm/sec)	Figure
1	0.50	3.28	29
5	0.51	3.35	30
10	0.63	4.14	31
15	0.63	4.14	32
20	0.63	4.14	33
25	0.63	4.14	34
30	0.63	4.14	35

The kinematic viscosity (ν) and the diffusion coefficient (D) needed in equation (9) were calculated in our laboratory for our test solution. The details of the calculation are shown in Appendices D and E respectively. The value of Sc was 4730. Table 10 summarizes the experimental local values of the mass transfer coefficients for electrode #5 (taken from Tables 6 to 9) and the literature-based local values calculated by equation (8). The values of the velocities needed in equation (8) were calculated and listed in Table 11 in Appendix A. A sample calculation of the literature-based local mass transfer coefficients (k) is shown in Appendix F.

For electrodes numbers 10, 15, 20, 25, and 30, the percent of agreement between the experimental local values of k obtained by scanning (Tables 7 to 9) and the literature-based local values obtained by equation (8) are: 65% at Re = 7174, 65% at Re = 10782, and 57% at Re = 14307. The large discrepancy between the experimental values and the literature-based values of k for all the electrodes is not surprising since equation (8) and other correlations found in the literature[27,28,65] have been developed for small molecules. Rigorous study, similar to that of Berger and Hau[69] needs to be established to develop correlations suitable for large molecules. These studies could be recommended for further research using our flow system.

TABLE 10

SUMMARY OF THE EXPERIMENTAL AND LITERATURE-BASED LOCAL MASS TRANSFER COEFFICIENTS (k) OBTAINED FOR ELECTRODE #5

Re	$kx10^3$ (cm/sec) Experimental		$kx10^3$ (cm/sec) Eqn. (8)	% Agreement*
	SSV	Scanning		
7174	2.43	2.63	1.00	59-62
10782	3.15	2.83	1.40	51-56
14307	3.48	3.35	1.80	46-48

*% Agreement = $\frac{\text{(Experimental - Eqn. 8) values}}{\text{Experimental values}}$

CHAPTER VI

CONCLUSION

The electrochemical technique was applied in the study of the mass transfer rates for macromolecules in a flow system. The direct oxidation of NADH (nicotinamide adenine dinucleotide, reduced) which represents a macromolecular substance (MW = 709.4) was studied in a rectangular duct. Glassy carbon disc electrodes were used as the working electrodes. Platinum sheet was used as the counter electrode and the reference electrode was Ag/AgCl.

The values of Re = 7174, 10782, and 14307 were used in this study. The value of Schmidt number (Sc) was 4730.

The steady state voltammetry (SSV) and scanning methods were used to obtain voltammograms. The SSV produced voltammograms with well defined mass transfer regions but the SSV was a slow and time consuming method. The scanning method was successfully used to obtain such voltammograms.

The experimental local mass transfer coefficients (k) were calculated from the limiting current values of the obtained voltammograms by the expression,

$$k = \frac{I_L}{nF\ A\ C_b} \qquad (6)$$

The experimental values of k were compared with the literature by using the correlation developed by Berger and Hau[65], which is valid for $8x10^3 < Re < 2x10^5$ and Schmidt number between 1000-6000. The correlation is,

$$St = \frac{k}{v} = 0.0165\ Re^{-0.14}\ Sc^{-0.67} \qquad (8)$$

Table 10 gives a summary of the experimental local values of k's and the literature-based values of k's. The discrepancy among these values of k's is due to the fact the correlation used as well as the others found in the literature have been developed for simple molecules[29,31].

The applications of our flow system with macromolecules are numerous. The local and average mass transfer rates with and without turbulence promoters and the development of correlations are such applications. The attachment of larger molecules (polylysine) to NADH will allow us to extend our studies to a homologans series of macromolecules.

Several recommendations have been submitted for our flow system that might help in any further study.

CHAPTER VII

RECOMMENDATIONS

The design and description of a flow system suitable for measuring the mass transfer rates for macromolecules has been presented. However, for the flow system to be widely applicable, I submit the following recommendations for further research:

A special electric circuit suitable for applying equal voltage ranges (-0.1 V to +.75 volts) to all electrodes in the flow cell is needed to enable us to study the local and overall mass transfer coefficient. The circuit built by Blank[94] can be modified and can be used with the SSV only. A similar circuit for scanning has to be constructed. The electronic system used by Leitz and Marincic[68] could be used for the scanning method.

The regeneration of NADH is necessary to save time and chemicals and to maintain constant concentration in the system. Several investigations[36,37,95] of such systems have been reported for flow rates up to 60 ml/min. Systems for higher flow rates are also needed.

The attachment of polylysine to NADH could be investigated to reveal the wide application of our flow system to larger molecules. Wills[74] has given details of attaching polylysine to NADPH.

The effects of turbulence promoters on mass transfer rates for macromolecular systems should also be studied using our flow system. Rigorous studies need to be established to develop correlations with and without turbulence promoters suitable for large molecules.

Also, for further studies, the glassy carbon electrodes could be chemically modified to enhance the reaction at the electrode surface. The studies cited in[96,97] show some methods for modifying carbon electrodes which could be utilized. One method is to chemically attach quinones to the surface of the carbon electrodes[96]. A second method is to chemically bond suitable enzymes (LDH and NAD) to the surface of the carbon electrodes[97].

The mechanical problem that we found with the counter electrode platinum sheet located downstream of electrode #5 should be investigated. Its effects should be eliminated before any further studies are conducted.

APPENDIX A

Calibration Curves

Figures 37 and 38 show the calibration curves for two rotameters, the first one with a maximum flow rate of 4 gal/min, and the second one with a maximum flow rate of 9.4 gal/min. Water is used as the working fluid, and the working temperature is 26°C.

Reynolds number

For our rectangular flow cell, Reynolds number N_{Re}, was calculated from the mean hydraulic radius, R_h [81],

$$R_h = \frac{S}{Z} \tag{10}$$

where S is the cross section of the stream in cm^2, and Z is the wetted perimeter in cm. The flow cell has a width (w) of 2.86 cm and a height (h) of 0.635 cm. The kinematic viscosity of water at 26°C is 0.87207×10^{-2} cm^2/sec,

$$R_h = \frac{wh}{2(w+h)} \tag{11}$$

and

$$N_{Re} = \frac{4R_h V}{\nu} \tag{12}$$

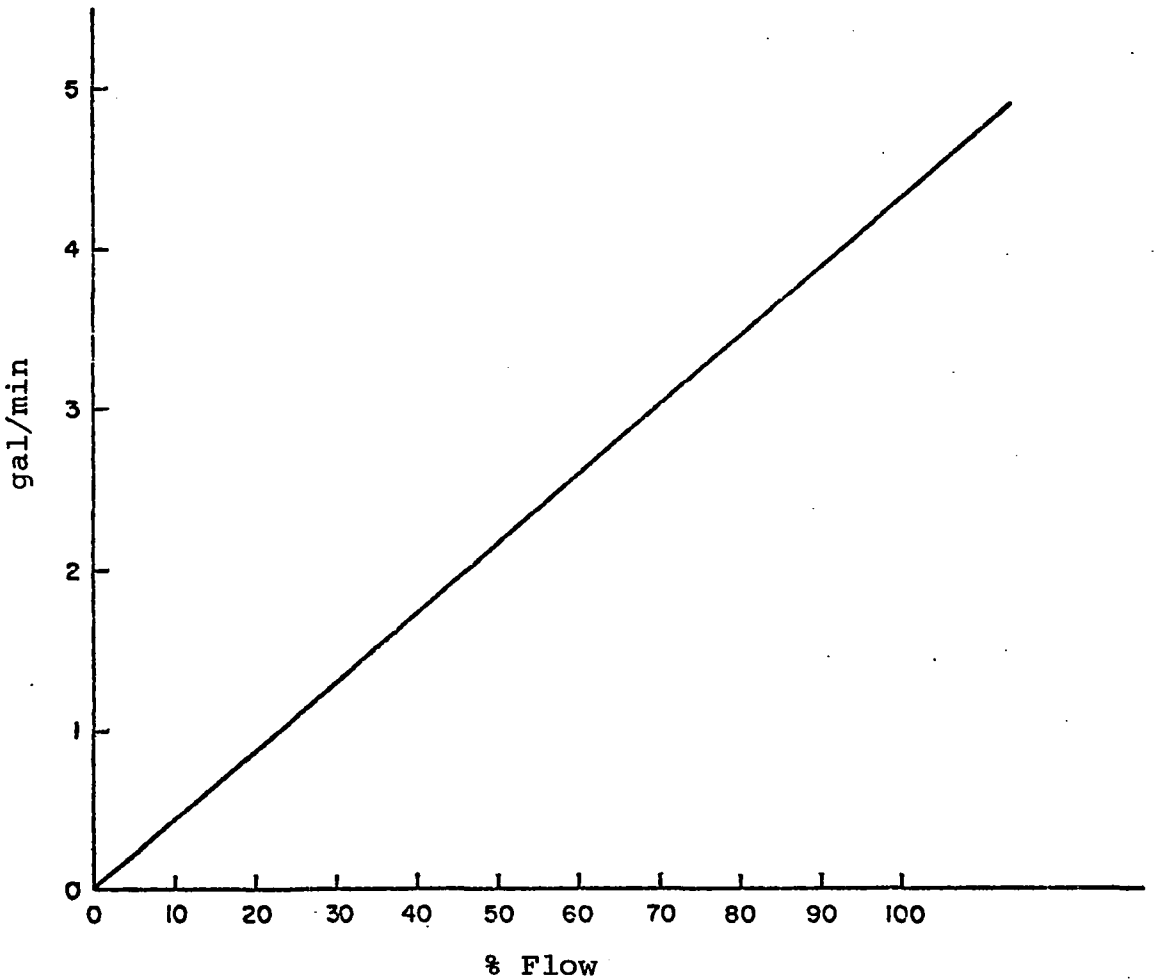

FIGURE 37. Calibration curve for rotameter of range up to 4 gal/min.

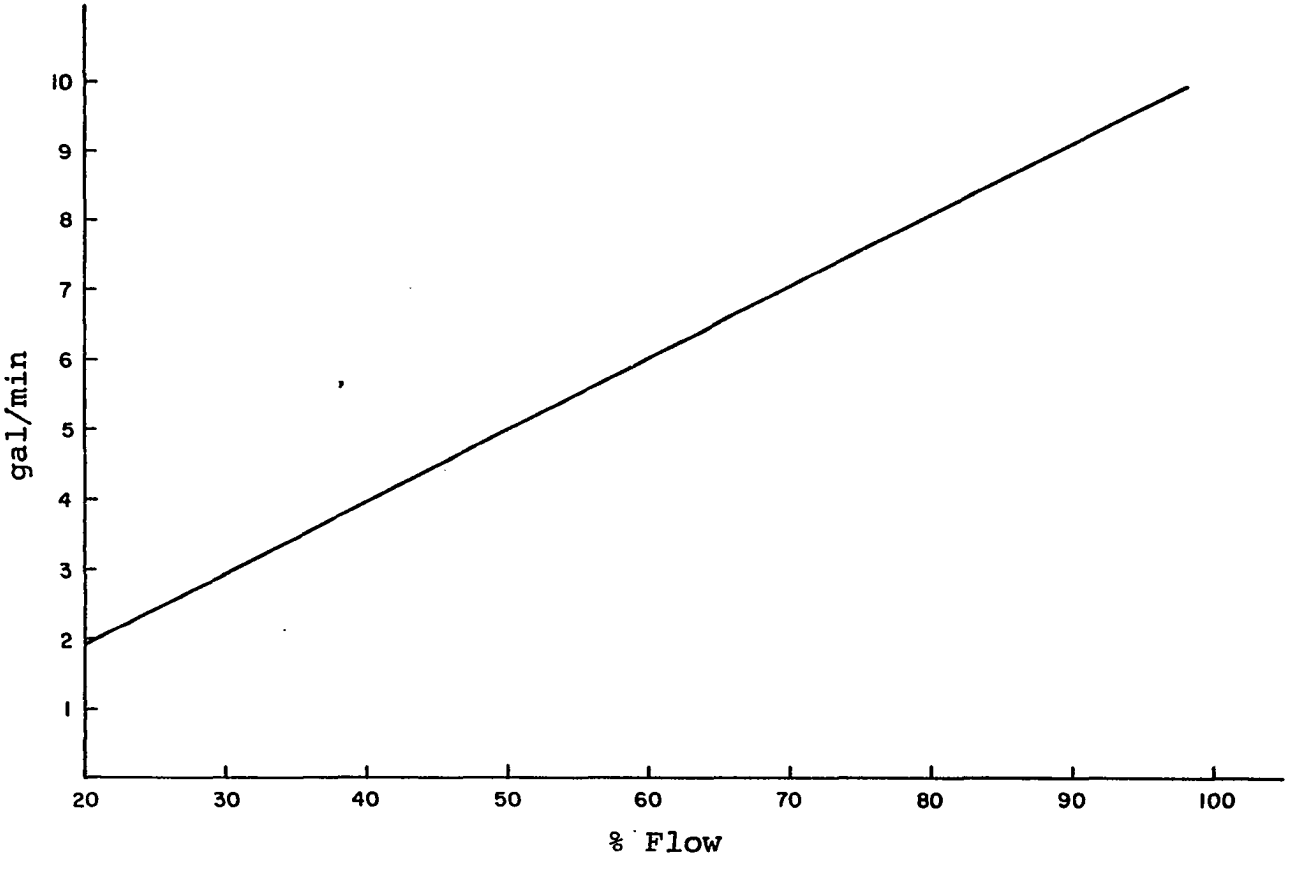

FIGURE 38. Calibration curve for rotameter of range up to 9.4 gal/min.

where V is the velocity in cm/sec and ν is the kinematic viscosity in cm^2/sec,

$$N_{Re} = \frac{4}{2} \left(\frac{wh}{w+h}\right) \frac{V}{\nu} \tag{13}$$

but the flow rate Q in cm^3/sec is

$$Q = VS = V(wh) \tag{14}$$

by combining equations 10 and 11, we get

$$N_{Re} = \frac{2Q}{(w+h)\nu} \tag{15}$$

To convert the measured value of Q from gal/min to cm^3/sec, multiply by 63.08333,

$$N_{Re} = \frac{(2)(63.08333)Q}{(2.86+0.635)(0.87207 \times 10^{-2})} \tag{16}$$

$$N_{Re} = 4148.9488Q \tag{17}$$

The four values of N_{Re} used in this study were calculated by equation (17), and listed in Table 11.

Velocity

The velocity at the calculated flow rates is found by

$$V = \frac{Q}{wh} \tag{18}$$

where Q in cm^3/sec, using the conversion factor 63.08333, we get

$$V = \frac{63.08333Q}{(2.86)(0.635)} \tag{19}$$

$$V = 34.7356Q \tag{20}$$

The corresponding four values of velocity V is calculated by equation (20), which is shown above. The results are shown in Table 11.

TABLE 11

SUMMARY OF COMPUTED N_{Re}, FLOW RATES, AND VELOCITIES AT 40%, 60%, 80% FLOW

% Flow	Q gal/min	N_{Re}	V cm/sec	Figure
40	1.73	7174	60.1	37
60	2.6	10782	90.3	37
80	3.45	14307	119.8	37
60	6	24882	208.4	38

APPENDIX B

Effective Area

To calculate the effective area of one of the glassy carbon electrodes, a current-time decay curve has been recorded for 3.88 mM of potassium ferrocyanide under linear diffusion (that is to say the quantity $(it)^{\frac{1}{2}}$ is a constant). Figure 39 shows the current-time curve for the ferrocyanide system. The Cottrell equation is

$$i = \frac{nF\ A\ D^{\frac{1}{2}}\ C_b}{(\pi t)^{\frac{1}{2}}} \qquad (21)$$

where i is the current in amperes, n is the number of electrodes involved in the reaction, A is the effective area in cm^2, C_b is the bulk concentration in moles per milliliters, t is time in seconds and D is the diffusion coefficient in cm^2/sec. The equation is rearranged and solved for A as follows;

$$A = \frac{i(\pi t)^{\frac{1}{2}}}{nF\ D^{\frac{1}{2}}\ C_b} \qquad (22)$$

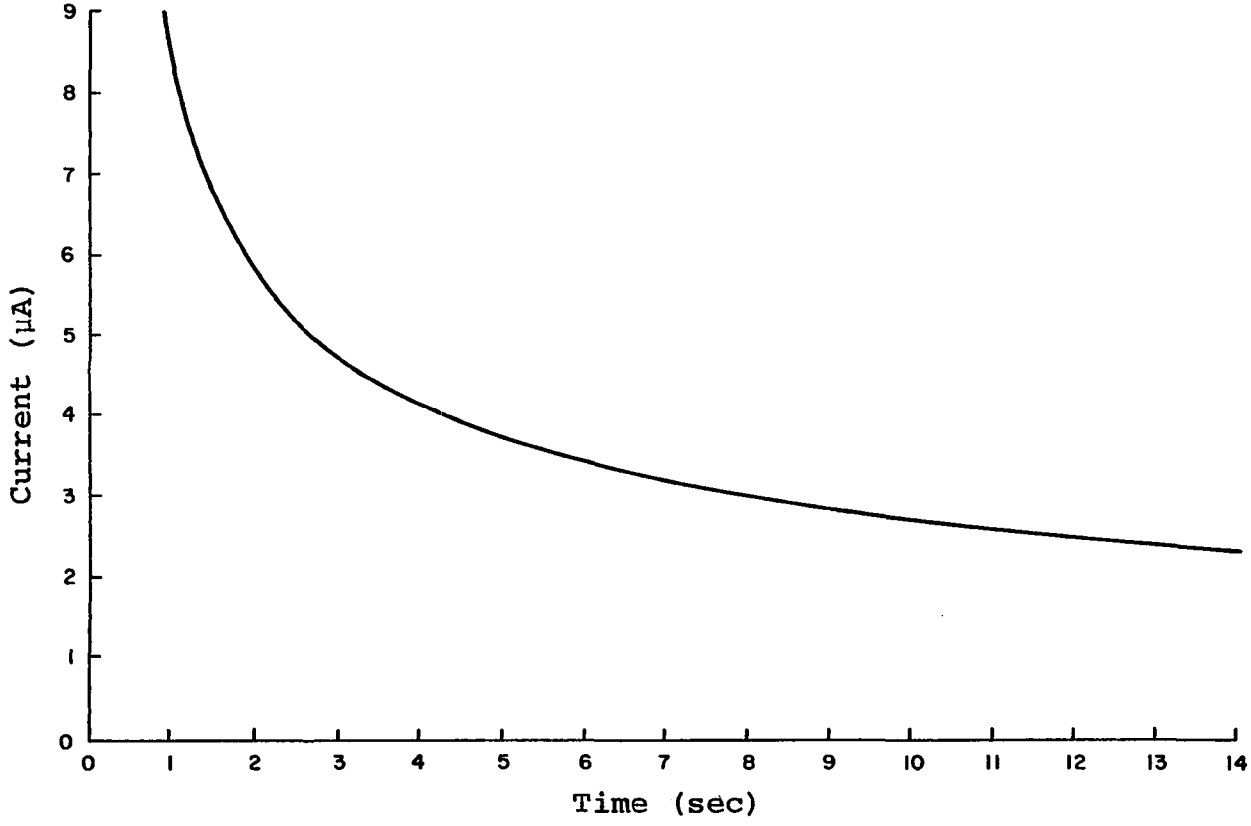

FIGURE 39. Current-time decay curve for effective area of a disc electrode.

The reaction is

$$Fe\ (CN)_6^{-4} \rightarrow Fe\ (CN)_6^{-3} + e \qquad (23)$$

The values of the known parameters in equation (22) are:

n(from equation 23) = 1

F, the Faraday = 96500 col/mole

C_b = 3.88×10^{-6} mol/mil

D = 6.29×10^{-6} cm^2/sec

The value of D is taken from Table 8-2 in Adams[78] for 1 MkCl which is equivalent to 3.88 mM for ferrocyanide. Therefore,

$$A = \frac{(\pi)^{\frac{1}{2}} \times 10^{-6}}{(1)(96500)(6.29\times10^{-6})^{\frac{1}{2}}(3.88\times10)} (i)(t)^{\frac{1}{2}}$$

$$A = 1.8875 \times 10^{-3}\ (i)(t)^{\frac{1}{2}} \qquad (24)$$

The current in expression (24) is in μA. This expression and Figure 39 are used to calculate the average area of the electrode surface. Table 12 summarizes the calculation of A. The value of $(it)^{\frac{1}{2}}$ is fairly constant between t = 5.5 sec. to t = 8 sec. The average value of A between 5.5 to 8 sec. is 0.0789 cm^2.

TABLE 12

EFFECTIVE AREA CALCULATION FOR GLASSY CARBON DISC ELECTRODE DETERMINED BY CURRENT-DECAY METHOD

Time (t) sec.	Current (i) μA	$(it)^{\frac{1}{2}}$	Area (A) cm^2
2.0	29	0.0076	0.07741
2.5	26	0.0081	0.07760
3.0	23.75	0.0084	0.07765
3.5	22.15	0.0088	0.07822
4.0	20.75	0.0091	0.07833
4.5	19.65	0.0094	0.07868
5.0	18.70	0.0097	0.07893
5.5	18.00	0.0099	0.07968
6.0	17.15	0.0101	0.07929
6.5	16.55	0.0104	0.07964
7.0	16.00	0.0106	0.07990
7.5	15.50	0.0108	0.08012
8.0	15.00	0.0110	0.08008

APPENDIX C

SAMPLE CALCULATION

Experimental Local Mass Transfer Coefficient

The experimental local mass transfer coefficient (k) was calculated from equation (6). One sample calculation based on the limiting current value (I_L) of Figure 11 is shown below,

$$k = \frac{I_L}{nF\ A\ C_b} \qquad (6)$$

where k is the local mass transfer coefficient in cm/sec, I_L is the limiting current value in amperes, n is the number of electrons involved in reaction (1), F is the Faraday, A is the electrode surface area in cm^2, and C_b is the bulk concentration in moles per cm^3. The value of the known parameters for equation (6) are:

$$I_L = 0.37\ \mu A = 0.37 \times 10^{-6}\ A = 0.37 \times 10^{-6}\ \text{col/sec.}$$

$$n\text{(from equa. 1)} = 2$$

$$F = 96500\ \text{col/mole}$$

$$C_b(\text{NADH}) = 10\mu M = 10\text{x}10^{-6}\ \text{mol/lit}$$
$$= 10\text{x}10^{-9}\ \text{mol/cm}^3$$

$$A\ (\text{from Appendix B}) = 0.0789\ \text{cm}^2$$

Therefore, the mass transfer coefficient using equation (6) was calculated as follows,

$$k\ [=]\ \frac{\frac{\text{col}}{\text{sec}} \left| \frac{\text{mol}}{\text{col}} \right| \frac{\quad}{\text{cm}^2} \left| \frac{\text{cm}^3}{\text{mol}} \right.}{} [=]\ \text{cm/sec} \qquad (25)$$

$$k = \frac{I_L}{(2)(96500)(.0789)(10\text{x}10^{-9})} \qquad (26)$$

$$k = \frac{I_L}{1.5228\text{x}10^{-4}} \qquad (27)$$

$$k = \frac{0.37\text{x}10^{-6}}{1.5228\text{x}10^{-4}}$$

$$k = 2.43\text{x}10^{-3}\ \text{cm/sec}$$

All values of local mass transfer coefficients for all limiting current values listed in Tables 1 to 4 were calculated by equation (27) and are shown in Tables 6 to 9.

APPENDIX D

Kinematic Viscosity Calculation

The kinematic viscosity(ν) for our test solution (.05M phosphate buffer + 10μM NADH + 20μM NAD^+, pH 9.2) was determined by using size 50 Cannon-Fenske viscometer. It was calibrated at 26°C with deionized water to give the following expression,

$$\nu = (3\text{x}10^{-5})t \qquad (28)$$

where ν is in cm^2/sec, and t is the flow time in seconds. For our test solution, the flow time was measured three times and the average flow time was found to be 315.32 seconds. The value of ν is

$$\nu = (3\text{x}10^{-5})(315.32)$$
$$\nu = 0.946\text{x}10^{-2}\ cm^2/sec.$$

APPENDIX E

Diffusion Coefficient Calculation

The diffusion coefficient (D) for our test solution (.05M phosphate buffer + 10μM NADH + 20μM NAD^+, pH 9.2) was determined by voltammetry at one of our glassy carbon disc electrodes. The same experimental set-up described by Blaedel and Jenkins[81] was used to obtain the limiting current at a rotating disc electrode. The limiting current was 0.34 μA at an RPM of 1000. The value of D was determined from the Levich equation cited in reference (73),

$$I_L = 1.5 \times 10^5 \; nA \; D^{2/3} \; \nu^{-1/6} \; N^{\frac{1}{2}} \; C_b \qquad (29)$$

where I_L is the limiting current in microamperes, n is the number of electrons involved in the reaction, A is the effective electrode area in cm^2, D is the diffusion coefficient in cm^2/sec, ν is the kinematic viscosity in cm^2/sec, N is the rotation rate of the electrode in revolutions per second, and C_b is the bulk concentration in millimoles per liter. The values of the known

parameters in equation (29) are:

n (from equation 1) = 2

A (from Appendix B) = 0.0789 cm^2

ν (from Appendix C) = 0.946×10^{-2} cm^2/sec

N = 1000 RPM = 16.7 RPS

C_b = 10μM = 10×10^{-3} millimolors/lit

I_L = 0.34μA

$$I_L = 1.5 \times 10^5 (2)(.0789)(D)^{2/3}(0.946 \times 10^{-2})^{-1/6}(N)^{\frac{1}{2}}(10 \times 10^{-3})$$

$$I_L = 523.53\ (D)^{2/3}\ N^{\frac{1}{2}} \qquad (30)$$

Solving for the diffusion coefficient D, we get

$$D = \left[\frac{I_L}{523.53\ N^{\frac{1}{2}}}\right]^{3/2} \qquad (31)$$

Substituting the value of I_L = 0.34μA and N = 16.7 RPS, in equation (31), we get

$$D = \left[\frac{0.34}{523.53\ (16.7)^{\frac{1}{2}}}\right]^{3/2}$$

$$D = 0.2 \times 10^{-5}\ cm^2/sec.$$

This value of D was also calculated with the limiting current value obtained by Blaedel and Jenkins[81]. The value of ν was not given by those investigators for their test solution (0.1M NaCl -0.00M phosphate buffer, pH 7.8). We used our measured value of ν since our test

solution is similar to the one used by Blaedel and Jenkins[81]. The value of I_L obtained by Blaedel and Jenkins[81] was 0.375μA at RPM = 1007. Substituting these two values of I_L = 0.375μA and N = 16.78 RPS in equation (31) we get,

$$D = \left[\frac{0.375}{523.53\ (16.78)^{\frac{1}{2}}}\right]^{3/2}$$

$$D = 0.23 \times 10^{-5}\ cm^2/sec$$

Schmakel et al[98] obtained the diffusion coefficient of NAD^+ and other biological compounds using pure water as a solvent. The value of D for NAD^+ was 0.55×10^{-5} cm^2/sec. This indicates that our value of D is of the same order of magnitude.

APPENDIX F

Sample Calculation for Local Mass Transfer Coefficient Based on the Literature Correlations

The local mass transfer coefficient (k) was calculated from the literature correlations of equation (8). One sample calculation, based on Re = 7171 and v = 60.1 cm/sec from Table 11 in Appendix A, is shown below,

$$St = \frac{k}{v} = 0.0165\ (Re)^{-0.14}\ (Sc)^{-0.67} \qquad (8)$$

where $$Sc = \frac{\nu}{D} \qquad (9)$$

$$= \frac{0.946 \times 10^{-2}}{0.2 \times 10^{-5}}$$

$$= 4730$$

Since the value of Sc is constant, equation (8) becomes

$$\frac{k}{v} = 0.0165\ (4730)^{-0.67}\ (Re)^{-0.14}$$

$$= 5.69 \times 10^{-5}\ (Re)^{-0.14} \qquad (32)$$

Substituting the value of Re = 7174 and v = 60.1 cm/sec in equation (32) we get,

$$\frac{k}{60.1} = 5.69\text{x}10^{-5} \ (7174)^{-0.14}$$

$$= 1.64\text{x}10^{-5}$$

and $$k = (1.64\text{x}10^{-5})(60.1)$$

$$k = 1.00\text{x}10^{-3}$$

The other values of k based on equation (8) at Re = 10782 and v = 90.3 cm/sec, and Re = 14307 and v = 119.8 cm/sec are listed in Table 10.

BIBLIOGRAPHY

1. Kunst, B., B. Arneri, Z. Vajnaht, Desalination 16, 169, (1975).

2. Agrawal, J.P., and S. Souriirajan, Ind. & Engr. Chem., Proc. Des. Devel. 8 (4), 439 (1969).

3. Jonsson, G. and C.E. Beosen, Desalination 17, 145 (1975).

4. Jonsson, G. and C.E. Boesen, Desalination 21, 1 (1977).

5. Murkes, J. and H. Bohman, Desalination 11, 269 (1972).

6. Brian, P.L.T., in Desalination by Reverse Osmosis, V. Merten, (Ed.), MIT Press, (1966) pp. 161-202.

7. Pusch, W., in Reverse Osmosis Membrane Research, H.K. Lonsdale and H.E. Podull, (Eds.), Plenum Press, New York (1972), pp. 43-60.

8. Blatt, W.F., A. Dravid, A.S. Michaels, L. Nelsen, in Membrane Science and Technology, J.E. Flinn, (Ed.), Plenum Press, New York (1970), pp. 47-97.

9. Goldsmith, R.L., Ind. Eng. Chem., Fund. 10, 113 (1971).

10. Michaels, A.S., L. Nelsen, M.C. Porter, in Membrane Processes in Industry and Biomedicine, M. Bier, (Ed.), Plenum Press, New York (1971), pp. 197-232.

11. Michaels, A.S., Chem. Engr. Progr. 64 (12), 31 (1968).

12. Merten, V., (Ed.), Desalination by Reverse Osmosis, The MIT Press, Cambridge, Massachusetts (1966).

13. Sourirajan, S., Reverse Osmosis, Academic Press, New York (1970).

14. Meares, P., (Ed.), Membrane Separation Processes, Elsevier, Amsterdam (1976).

15. Porter, M.C. and L. Nelsen, in Recent Developments in Separation Science, Vol. 2, Li, N.N., (Ed.), CRC Press, Cleveland (1972), pp. 227-267.

16. Bier, M., (Ed.), Membrane Processes in Industry and Biomedicine, Plenum Press, New York (1971).

17. Lacey, R.E. and S. Loeb, (Eds.), Industrial Processing with Membranes, Wiley-Interscience, New York (1972).

18. Flinn, J.E., (Ed.), Membrane Science and Technology, Plenum Press, New York (1970).

19. Van Oss, C.J., in Techniques of Surface and Colloid Chemistry and Physics, Vol. 1, Good, R.J., R.R. Stromberg, R.L. Patrick, (Eds.), Marcel Decker, Inc., New York, (1972), pp. 89-110.

20. Blatt, W.F., Methods in Enzymology 22, 39 (1971).

21. Smith, K.A., C.K. Colton, E.W. Merrill, L.B. Evans, CEP Symposium Series 64 (84), 45 (1968).

22. Babb, A.L., C.J. Maurer, D.L. Fry, R.P. Popovich, R.E. McKee, CEP Symposium Series 64 (84), 59 (1968).

23. Kauffman, T.G. and E.F. Leonard, AIChE J. 14 (3), 421 (1968).

24. Colton, C.K., K.A. Smith, E.W. Merrill, P.C. Farrell, J. Biomed Mater. Res. 5, 459 (1971).

25. Gotch, F.A., J. Autlan, C.K. Colton, H.E. Ginon, B.J. Lipps, E. Lowrie, The Evaluation of Hemodialyzers, DHEW Publication No. (NIH) 72-103, (1971).

26. Gill, W.N., L.J. Derzansky, and M.R. Doshi, in Surface and Colloid Science, Vol. 4, E. Matjevic, (Ed.), Wiley-Interscience, New York (1971), pp. 261-360.

27. Murkes, J. and H. Bohman, Desalination 11, 269 (1972).

28. Hwang, S.T. and K. Kammermeyer, Membranes in Separations, Wiley-Interscience, New York (1975).

29. de Fillippis, R.P. and R.L. Goldsmith, in Membrane Science and Technology, J.E. Flinn, (Ed.), Plenum Press, New York (1970), pp. 33-46.

30. Goldsmith, R.L., R.P. de Flippl, S. Hossain, R.S. Timmins, in Membrane Processes in Industry and Biomedicine, M. Bier (Ed.), Plenum Press, New York (1971), pp. 267-300.

31. Porter, M.C., Ind. & Engr. Chem., Prod. Res. Develop. 11, (3), 234 (1972).

32. Bailey, J.E. and D.F. Ollis, Biochemical Engineering Fundamentals, McGraw-Hill, New York (1977).

33. Wingard, L.B., et. al., Applied Biochemistry and Bioengineering, Leon Goldstein: Academic Press, New York (1972).

34. Kobyayashi, T. and K.J. Laidler, Biotechnol. Bioeng. 16 (1-6), 99 (1974).

35. Chi-Sing Tse, D. and T. Kuwana, Anal. Chem. 50 (9), 1315 (1978).

36. Coughlin, R.W. and B.F. Alexander, Biotechnol. Bioeng. 17, 1379 (1975).

37. Malinauskas, A.A. and J.J. Kulys, Biotechnol. Bioeng. 21, 513 (1979).

38. Malinauskas, A.A. and J.J. Kulys, Anal. Chim. Acta. 98, 31 (1978).

39. Middleman, S., Transport Phenomena in Cardiovascular Systems, John Wiley, New York (1972).

40. Harriot, P., and R.M. Hamitton, Chem. Engr. Sci. 20, 1073 (1965).

41. Mishra, P., I.M. Mishra, T.N. Singh and S.N. Upadhyay, Indian Chem. Engr. 17 (2), 30-33 (1975).

42. Upadhyay, S.N., M. Singh, P.N. Dwivedi, and G. Tripathi, Chem. & Engr. Data 21 (2), 144 (1976).

43. Beg, S.A., Warme and Stuffubertragung 6 (1), 45-51 (1973).

44. Linton, W.H. and T.K. Sherwood, Chem. Engr. Progr. 46, 258 (1950).

45. Thomas, D.G., AIChE J. 11 (3), 520 (1965).

46. MacLeod, N., and G. Stewart, Chem. Engr. Sci. 12, 142 (1960).

47. MacLeod, N., M.D. Cox and R.B. Rodd, Chem. Engr. Sci. 17, 923 (1962).

48. McLeod, N. and R.B. Todd, Int. J. Heat Mass Transfer 16, 485 (1973).

49. Masliyah, J.H., and T.T. Nguyen, Can J. Chem. Eng. 54, 299 (1976).

50. Kapur, D.N. and N. MacLeod, Nature, Phys. Sci. Lond. 237, 57 (1972).

51. Kapur, D.N. and N. MacLeod, Int. J. Heat Mass Transfer 17, 1151 (1974).

52. Kapur, D.N. and N. MacLeod, AIChE J. 21 (1), 184 (1975).

53. Masliyah, J.H. and T.T. Nguyen, Canada J. Chem. Eng. 54, 299 (1976).

54. Wild, H.G. and J. Uhlenbusch, Int. J. Heat Mass Transfer 21, 677 (1978).

55. Koncar-Djurdjevic, S. Nature 172, 858 (1953).

56. Cvijović, S.D. and M.V. Mitrovic, Bull. Soc. Chem. Biograd., 34 453 (1969).

57. Koncar-Djurdjevic, S.K. and A.P. Dudkovic, AIChE J. 23, 125 (1977).

58. Koncar-Djurdjevic, S.K. and A.P. Dudkovic, AIChE J. 25 (5), 895 (1979).

59. Koncar-Djurdjevic, S.K. and A.P. Dudkovic, AIChE J. 26 (2), 299 (1980).

60. Lin, C.S., E.B. Denton, H.S. Caskill and G.L. Putnam, Ind. & Engr. Chem. 43 (9), 2136 (1951).

61. Reiss, L.P. and R.J. Hanratty, AIChE J. 8 (2), 245 (1951).

62. Van Shaw, P., L.P. Reiss and T.J. Hanratty, AIChE J. 9 (3), 362 (1963).

63. Hubbard, D.W. and E.N. Lightfoot, Ind. & Eng. Chem. Fundamentals 5, 370 (1966).

64. Shaw, D.A. and T.J. Hanratty, AIChE J. 23 (1), 28 (1977).

65. Berger, F.P. and K.-F. F.-L. Hau, Int. J. Heat Mass Transfer 20, 1185 (1977).

66. Mizushina, T., Adv. Heat Transfer 7, 87 (1971).

67. Watson, J.S. and D.G. Thomas, AIChE J. 13 (4), 676 (1967).

68. Leitz, F.B. and L. Marincis, Applied Electrochem. J. 7, 473 (1977).

69. Strock, A. and F. Coeuret, Electrochimica Acta 22, 1155 (1976).

70. Sidahmed, G.H. and R.G. Griskey, AIChE J. 18 (1), 138 (1972).

71. Butson, J. and D.H. Glass, Int. Conf. on Drag Reduction, 4th-6th, A3-41 to A3-61 (1974).

72. McConaghy, G.A. and T.J. Hanratty, AIChE J. 23 (4), 493 (1977).

73. Dryhurst, G., Electrochemistry of Biological Molecules, Academic Press, New York (1977).

74. Wills, R.A., Ph.D. Dissertation, University of Oklahoma (1978).

75. Luduc, P. and D. Thevenot, Bioelectrochem. Bioenergetics 1, 96 (1974).

76. Elving, P.J., et al., J. Am. Chem. Soc. 97 (10), 2591 (1975).

77. Thomas, L.C. and G.D. Christian, Analytica Chemica Acta, 78, 271 (1975).

78. Charles, M., et al., Biochemica et Biophysica Acta 385, 362-370 (1975).

79. Coughlin, R.W., et al., Biotechnol. Bioeng. 19, 901 (1977).

80. Blaedel, W.J. and R.A. Jenkins, Anal. Chem. 46 (13), 1952 (1974).

81. Blaedel, W.J. and R.A. Jenkins, Anal. Chem. 47 (8), 1337 (1975).

82. Moiroux, J. and P.J. Elving, Anal. Chem. 50 (8), 1056 (1978).

83. Moiroux, J. and P.J. Elving, Anal. Chem. 51 (3), 346 (1979).

84. Adams, R.N., Electrochemistry at Solid Electrodes, Marcel Dekker, New York (1969).

85. Delahoy, P., New Instrumental Methods in Electrochemistry, Interscience Publisher, New York (1954).

86. Newman, J.S., Electrochemical Systems, Prentice-Hall, Englewood Cliffs, New Jersey (1973).

87. Bird, R.B., W.E. Stewart and E.N. Lightfoot, Transport Phenomena, John Wiley & Sons, Inc., New York (1960).

88. Treybal, R.E., Mass Transfer Operations, McGraw-Hill, New York (1968).

89. Youngquist, G.R., Chemical Engr. Educ. 13 (1), 20 (1979).

90. Berger, F.P. and A.W. Whitehead, J. Brit. Nucl. Energy Soc. 16, 153 (1977).

91. Dryhurst, G., Class notes on Electroanalytical Chemistry, at the University of Oklahoma (1980).

92. Personal communication between L. Karber, one of Dr. Dryhurst's graduate students, and the author of this study, September 15, 1980.

93. Personal communication between Dr. G. Dryhurst and the author of this study, September 18, 1980.

94. Blank, C.L., J. Chromatogr. 117, 35 (1976).

95. Orelaja, V.O., Master Thesis, The University of Oklahoma (1976).

96. Chi-Sing Tse, D. and T. Kuwana, Anal. Chem. 50 (9), 1315 (1978).

97. Smith, M.D. and C.L. Olson, Anal. Chem. 46 (11), 1544 (1974).

98. Santhanam, K.S.V., C.O. Scmakel and P.J. Elving, Bioelectrochem. Bioeng. 1, 147 (1974).